BOBCATS ACROSS THEIR GEOGRAPHIC RANGE: COMBINING ECOLOGICAL NICHE MODELING AND MORPHOLOGY TO ASSESS THE POPULATION GENETIC STRUCTURE OF *LYNX RUFUS*

By

ALLISON MARCELLA LOVELESS

Bachelor of Science in Geography/Environmental Studies

University of California, Los Angeles

Los Angeles, California

2009

Submitted to the Faculty of the
Graduate College of the
Oklahoma State University
in partial fulfillment of
the requirements for
the Degree of
MASTER OF SCIENCE
December, 2014

BOBCATS ACROSS THEIR GEOGRAPHIC RANGE: COMBINING ECOLOGICAL NICHE MODELING AND MORPHOLOGY TO ASSESS THE POPULATION GENETIC STRUCTURE OF *LYNX RUFUS*

Thesis Approved:

Monica Papeş

Thesis Adviser

Karen McBee

Michael Tobler

ACKNOWLEDGEMENTS

This work would not have been possible without the support and contributions made by numerous colleagues and researchers. First and foremost, thanks to my research advisor, M. Papeş, for her instruction, suggestions, and support. Thanks to D. M. Reding and P. M. Kapfer for their data contributions. I would also like to thank my committee members: M. Tobler and K. McBee, of Oklahoma State University, whose ideas and instruction were of immeasurable value. K. Weller designed and constructed the apparatus used to collect skull images, and Á. S. Nyári who put the finishing touches on the image apparatus and provided statistical method instruction. Thanks to R. M. Timm at the University of Kansas Biodiversity Institute and S. Peurach at the Smithsonian National Museum of Natural History for hosting and aiding my collection of specimen images and information. Finally, thank you to all of my wonderful colleagues at Oklahoma State University, X. Feng, I. Gherghel, F. Gebresenbet, C. Walker, R. Pandi, and E. Capps, for their support, advice, and friendship during this project and my graduate program.

Name: ALLISON MARCELLA LOVELESS

Date of Degree: DECEMBER, 2014

Title of Study: BOBCATS ACROSS THEIR GEOGRAPHIC RANGE: COMBINING ECOLOGICAL NICHE MODELING AND MORPHOLOGY TO ASSESS THE POPULATION GENETIC STRUCTURE OF *LYNX RUFUS*

Major Field: ZOOLOGY

Abstract: Despite a broad distribution, general habitat requirements, and long dispersal potentials, bobcats (*Lynx rufus*) exhibit a genetic division that longitudinally transects central North America. I investigated whether (1) the climate of the Last Glacial Maximum (LGM, 21 ka) isolated bobcats into refugia and whether current climate results in reduced gene flow between the segregate populations, and (2) geographic and climatic patterns in cranial morphology reflect population identity. I created ecological niche models to evaluate climatic suitability under historical (LGM) and contemporary conditions, and used two-dimensional geometric morphometric methods to evaluate variations in the cranium and mandible of *L. rufus* across its geographic range. The ecological niche models support a genetic disparity along a longitudinal gradient in the central North America. Models projected onto LGM climate reconstructions provided evidence of increased suitability in the northwest and southeast portions of their range and decreased suitability in the central U.S. that may have created refugia in western and eastern North America during the LGM. Morphological analyses identified a significant linear trend across a longitudinal gradient rather than distinct morphological divergence between lineages. In addition, correlations of morphologies with the principle components of climate variables revealed that precipitation and temperature are most significant predictors of morphological diversity in bobcats. My models suggest that the contemporary Great Plains ecoregion may be restricting bobcat migration and gene flow, effectively maintaining disparate genetic populations. Morphological analyses show that environmental variation may be a larger contributing factor to phenotypic variation than is population identity. By estimating the contemporary and LGM geographic distributions, and quantifying local adaptations, I provided a robust assessment of the biogeographic considerations for population genetic structure of bobcats.

TABLE OF CONTENTS

Page

LIST OF TABLES

LIST OF FIGURES

Figure Page

BOBCATS ACROSS THEIR GEOGRAPHIC RANGE: COMBINING ECOLOGICAL NICHE MODELING AND MORPHOLOGY TO ASSESS THE POPULATION GENETIC STRUCTURE OF *LYNX RUFUS*

INTRODUCTION

Cryptic population structure – the presence of genetic subdivision without obvious barriers to gene flow – is a subject of continued interest among researchers and recent studies have revealed the presence of complex genetic structures in many wide ranging species (e.g., Sacks et al., 2004; Pilot et al., 2006; Latch et al., 2014). The purported mechanisms of divergence are varied, and may include ecological and historical factors, as well as topographic features that may span either or both time frame. For example, physical barriers such as mountain ranges (Rueness et al., 2003), water features (Millions et al., 2007), man-made structures (Riley et al., 2006), or habitat degradation (Haag et al., 2010) can limit gene flow across a species range. More subtle drivers of genetic differentiation may include social and behavioral dynamics such as dietary niche preferences (Pilot et al., 2012), and dispersal patterns (Sacks et al., 2005). Furthermore, historical climate processes such as glaciation cycles and associated vegetation shifts, can leave a lasting mark on the current genetic structure of many species (Wooding et al., 1997). With contemporary genetic and distribution data alone, however, it can be challenging to discern the relative contributions of historical vicariance events and ongoing ecological processes. Moreover, without phenotypic data

or adaptive genetic markers, it can be difficult to determine the importance of selective and neutral processes in shaping variation in natural populations. Thus, combining multiple sources of data – including DNA, environmental and climatic variables, and phenotypic data – can provide greater insight into the nature of cryptic population subdivision (Pease et al., 2009; Fordham et al., 2014).

A large scale genetic study of bobcats (*Lynx rufus*) conducted by Reding et al. (2012) provides the basis for the climatic and morphological assessment of their population genetic structure presented here. *Lynx rufus* are terrestrial, mid–sized carnivores that are distributed continuously across the contiguous United States, northern and central Mexico, and southern Canada (Hansen, 2007). This range consists of broad ecological variants, from the cold forests of the northeastern U.S. and southern Canada, to the North American deserts, the tropical humid forests of Florida, and the dry scrubland of central Mexico (Commission for Environmental Cooperation, 1997). *Lynx rufus* is primarily a solitary species with large potential dispersal distances (Hansen, 2007). Prey preferences, associated activity patterns, home range areas, and pelage variations are strongly correlated with geographic location, topography, sex, and even seasonality (Hansen, 2007). This species' crepuscular and nocturnal activity patterns are also strongly associated with the activity patterns of their prey (Wilson et al., 2009). In general, bobcats residing in southern North America prey primarily on lagomorph species and occupy relatively small ranges; in Mississippi winter months, males inhabit 7.32 km^2 while females are more restricted, roaming only 3.33 km^2 (Chamberlain et al., 2003). Alternatively, in northern latitudes where small prey can be scarce, bobcats may kill ungulate species such as white – tailed deer (*Odocoileus virginianus*) and mule deer

(*Odocoileus hemionus*; Hansen, 2007; Wilson et al., 2009). At these high latitudes, home ranges as large as 112 km^2 (Litvaitis et al., 1987) and high elevation ranges of up to 325 km^2 have been documented (Fox, 1990). Moreover, a single individual may disperse between 1 and 200 km during its life time, although females generally procure home ranges near or within their natal range (Davis et al., 2004). In addition to latitudinal variation in diet, combined studies have also show that diet diversity increases from east to west (e. g., Story et al., 1982; McLean et al., 2005), associated with longitudinal increases in the diversity of species (Badgley et al., 2000). Both mitochondrial DNA (mtDNA) haplotype network and microsatellite analyses supported a genetic differentiation along a longitudinal transect in central North America (Reding et al., 2012). Phylogenetic analyses have also revealed the presence of ancestral haplotypes that suggest the contemporary lineages descended from refugia located in the northwestern and southeastern regions of North America, following recession of the last glacial maximum (LGM, 21 ka; Reding et al., 2012). However, the genetic boundary located in the Great Plains also coincides with a sharp transition in current environmental and ecological conditions. Thus, an intriguing question remains about whether the genetic boundary merely reflects a contact zone between historically isolated populations that have since expanded in range, or if ongoing processes are contributing to their separation. Additionally, evidence from phylogeographic, phylogenetic, and ecological research suggests that historical climate processes (glacial cycles) and current environmental conditions had a crucial influence in creating and maintaining current genetic and spatial distribution patterns within the Family Felidae as a whole (e. g., Mattern and McLennan, 2000; Reding et al., 2012).

Areas of contact and hybridization of distinct populations, such as is seen bisecting the range of bobcats, are called convergence or suture zones and are distinguished by regions of recent environmental transformation such as the removal of anthropogenic influence or variations in climate, and are characterized by geographic or environmentally unique features (Remington, 1968; Swenson and Howard, 2005). Remington (1968) suggested that the central Great Plains ecoregion represents a zone of secondary contact for many mammalian species that were isolated during the LGM. Additionally, possible aridification of this region during the Pleistoncene epoch may have created a more persistent barrier to dispersal that has only recently been colonized (Remington, 1968). Today the central Great Plains ecoregion is dominated by agriculture, grasslands, and prairies, and with rainfall increasing from west to east following the rain shadow of the Rocky Mountains and separating the humid forest of the eastern U.S. from the more diverse climates and topography of the west (Commission for Environmental Cooperation, 1997). The present study is one of few (e. g., Soberón and Martínez-Gordillo, 2012) to combine ecological niche modeling, supported by morphological analyses, to investigate the effect of climate on the niche of a species. This study also evaluated contemporary and historical distributions of *L. rufus* to seek evidence of historical isolation and contemporary restrictions of gene flow.

The goals of this study were to determine whether (1) climate of the LGM (21 ka) may have isolated bobcats into genetic refugia and whether current climate results in reduced gene flow between the segregate populations, and (2) cranial variation reflects genetic population identity or displays geographic patterns associated with climatic variation. I used ecological niche models (ENMs) to estimate the geographic regions with

suitable climatic conditions for species' survival (Soberón and Peterson, 2005; Jimenez-Valverde, 2012). Even more powerful in combination with genetic information, a niche model can discern environmental influences on the development and maintenance of a population's distribution and genetic structure, thus the underlining ecological causes of spatial organization (Kozak et al., 2008). Morphology can tell us yet another side of the story. Traditional linear morphometric research has determined phenotypic variation within *L. rufus* at regional and local scales throughout the U.S. (e. g., Rolley, 1983, Sikes and Kennedy, 1992; Wigginton and Dobson, 1999; Wilson et al., 2009). In the present study I used two–dimensional geometric morphometric analyses to assess changes in skull shape of *L. rufus* in support of an east, west genetic cline and as a potential assessment of the biotic interaction of this species (e. g., Soberón and Martínez-Gordillo, 2012).

METHODS

1. **Evolution and maintenance of population genetic structure**:

Data acquisition

I collected a total of 965 specimen localities from the Mammal Networked Information System (MaNIS), the Oklahoma State University Collection of Vertebrates (OSU COV), and from previous research projects on genetic structure (Reding et al., 2012) and distribution of bobcats in the upper Midwest (Kapfer and Potts, 2012). Using location descriptions, I assigned geographic coordinates to the specimens with the applications GEOLocate (available at: http://www.museum.tulane.edu/geolocate/) and Google Earth (available at: http://www.google.com/earth/index.html). GEOLocate provides an error distance that represents the uncertainty of georeferenced localities. I

used only occurrences with a maximum uncertainty of 5 km. To avoid the over representation of one environmental region or condition, I subsampled the dataset based on the density of point occurrences within each U.S. level III EPA ecoregion (Western Ecology Division, 2013). Level III EPA ecoregions are distinguished at the ecosystem level according to physical, biological, and human influences. Such categories include terrain, climate, vegetation, wildlife, hydrology, human activities and land use, and geographic location (Commission of Environmental Cooperation, 1997). I used ArcGIS to calculate the average density of records for each ecoregion and those that exceeded the average were randomly subsampled to comply with the determined average.

I collected climate data to use as explanatory variables in ENMs. I downloaded climate data with a 2.5 arc minute resolution (4.5 km) available from the WorldClim database (Hijmans et al., 2005; available at: www.worldclim.org). Current climate conditions (1950 – 2000) were represented by 19 bioclimatic layers and elevation. These bioclimatic parameters represent biologically meaningful characteristics of climate change: annual and diurnal variations (e. g., mean diurnal temperature and annual mean temperature), properties of seasonality (e. g., range in annual precipitation and temperature), and extreme climate conditions (e. g., precipitation of the wettest and driest months, maximum temperature of the hottest month, and minimum temperature of the coldest month). The LGM climate dataset was produced by the Paleoclimate Modelling Intercomparison Project Phase II ($PMIP_2$; available at: http://pmip2.lsce.ipsl.fr/; Harrison et al., 2002; Braconnot et al., 2004) and was also downloaded from the WorldClim database (Hijmans et al., 2005). The $PMIP_2$ uses climate system feedbacks (atmosphere, ocean, land - surface, sea and land ice) to downscale (create a finer data resolution)

present WorldClim variables to produce the historic climate dataset. These data were also downloaded at a 2.5 arc minute resolution.

For consistency with current climatic data, I used only specimens collected from 1950 -2000 to train the models (model calibration). An external testing dataset (model validation) was generated using occurrences collected outside of this timeframe, in addition to points that exceeded the average occurrence density within each ecoregion. Prior selection of training and testing points allows maximization of occurrence data used to generate the models.

Model generation

I generated separate models for east and west lineages to evaluate the effect of climate on the geographic distributions under contemporary and LGM climates. The models were based on point localities I separated into east and west datasets in ArcGIS using an on-screen digitized line that best represented the haplotype structure of the occurrence data, with reference to the longitudinal cline created by Reding et al. (2012). The final training and testing datasets contained 231 training and 237 testing points for west partition and 248 training and 249 testing points for the east partition (Fig. 1).

For comparison, I created ENMs using two common algorithms: maximum entropy (Maxent; Phillips et al. 2008) and the Genetic Algorithm for Rule-Set Production (GARP). Maxent calculates the maximum likelihood probability given Gibbs probability distribution based on presence data and input climatic constraint layers (Soberón and Peterson, 2005; Phillips et al., 2008). GARP uses rules (atomic, logistic regression, bioclimatic envelope, negated bioclimatic envelope) to find correlations between presence, absence, and bioclimatic variables to build distribution predictions

(http://www.nhm.ku.edu/desktopgarp/UsersManual.html#intro). To avoid collinearity in the dataset (Dormann et al., 2012), I selected four sets of variables comprised from the 19 bioclimatic variables and elevation based on training region correlation analyses ($r^2 < 0.7$) and a distance based redundancy analysis (Reding et al., 2012) that determined precipitation of the warmest quarter as the most important climatic factor in the spatial genetic pattern (Table 1). For consistency, the same variable sets were used to generate east and west models. I created present day models and projected them onto climate data-sets of the LGM (21 ka). As training regions, I used the east and west portions of the range of *L. rufus* corresponding to each genetic population, representing the known distribution of each lineage, to eliminate background sampling (climate sampling) beyond the known geographic extent of each lineage. Additionally, Maxent generates a spatial estimation of the most dissimilar variable (MoD), in other words, the variable whose value at that point in geographic space is the most different from the conditions within the training region, thus the most influential in limiting the model prediction at that locality. This discriminating analysis enabled me to discern the variables associated with a cryptic climatic barrier inhibiting genetic dispersal. All models were run at a 2.5 arc minute resolution.

I evaluated the accuracy of all Maxent and GARP models using testing data to calculate the area under the receiver operating characteristic curve (ROC AUC) and partial testing AUC and associated z statistic for significance, respectively. The ROC curve plots the sensitivity (i.e., presence records predicted present) of a model against the proportion of study area predicted as present, in the implementation for presence – background modeling algorithms (Jimenez-Valverde, 2012). The area under this curve

represents the overall model performance with a value of 0.5 indicating a model that predicts presence with random accuracy. Although ROC AUC values are both species and region specific, thus difficult to compare across geographic areas, better model evaluation can be achieved by reporting these values in association with rates of testing omission error (presences that are predicted absent; Jimenez-Valverde, 2012). Omission error calculations require conversion of the continuous model output values (probability of suitability) to binary (presence – absence). I used a threshold of 10% omission of training points for this conversion which assumes some error in presence localities may have occurred during georeferencing or field collection. Thus the testing data omission error was calculated at the 10th percentile training presence threshold. The percent overlap between east and west lineage suitability predictions was calculated for each of the four models obtained with the different climate sets and averaged. Consensus models were created to display a degree of suitability for each population (area predicted present by 0 – 4 models) over the geographic extent of the combined training regions. The LGM models were additionally clipped to exclude the known extent of the Laurentide ice sheet that covered the majority of Canada and possibly as far south as 40°N during the Late Wisconsin glacial cycle of the Pleistocene, lasting from approximately 24 ka to 18 ka, since this likely posed a geographic barrier to dispersal for the bobcat (Ehlers and Gibbard, 2007; Reding et al., 2012).

2. **A morphological shape analysis of cranial variation in *Lynx rufus***:

Samples

I evaluated variations in skull shape and size across geographic distance using two-dimensional landmark based geometric morphometric methods (Zelditch et al.,

2004). A total of 218 skull specimens were collected from the University of Kansas Biodiversity Institute, Smithsonian National Museum of Natural History, and Oklahoma State University Collection of Vertebrates, and were photographed at three angles: lateral cranium (LC), ventral cranium (VC), and lateral mandible (LM). All images were collected by the same person (AML) using a Canon model G15 camera and a custom–made image apparatus that allowed the standardization of specimen orientation and camera distance. The lateral view of the cranium was acquired by orienting the sagittal plane of the skull parallel to the photographic plane. The ventral angle of the cranium was obtained by manipulating the palatine to be parallel to the photographic plane. The lateral angle of the mandible was acquired by orienting the long axis of the dentary parallel to the photographic plane. I sampled only complete skull specimens with known sex and locality information, and georeferenced to no more than 20 km error distances by the methods described in the previous objective. I assumed that the eruption of permanent teeth indicated fully developed individuals, thus only skulls with complete eruption of permanent teeth were sampled and those specimens determined to be very old, based on reference to cranial features described by Schmidly and Read (1986) and Garcia-Perea (1996), were excluded. From a trial analysis used to test the consistency of specimen orientation and landmark placement, I concluded that any variation due to human error was insignificant and was disregarded for the remainder of the study (Appendix S1).

Geographic and climate correlations of cranial shape and size change

I used tpsDig2 version 2.17 (Rolf, 2004; available at: http://life.bio.sunysb.edu/morph/) to digitize landmarks on each angle of the cranium and dentary separately and included two reference landmarks set on a standardized ruler to

correct for possible inconsistencies in camera distance. A total of 35 landmarks were set on the VC, 12 on the LC, and 9 on the LM (Appendix S2). The landmarks were chosen with reference to *Animal Skulls: a guide to North American species* (Elbroch, 2006) and geographic and morphometric studies of felids and other mammalian species conducted using traditional and geometric morphometric approaches (e. g., Sikes and Kennedy, 1992; Wigginton and Dobson, 1999; Marcus et al., 2000; Tanner et al., 2010). Homologous landmarks were placed bilaterally across the midline of the ventral cranium and averaged using the program MorphoJ version 1.05f (Klingenberg, 2011) as an additional step to remove error associated with specimen orientation and landmark placement.

The size of the specimen in relation to the distance of the camera was corrected for each set of coordinates using the Pythagorean Theorem. The landmarks were then overlaid by a generalized least squares Procrustes superimposition (Rohlf and Slice, 1990) in tps relative warp version 1.49 (tpsRelw; Rohlf, 2004; available at: http://life.bio.sunysb.edu/morph/). Procrustes superimposition method removes variation due to the rotation, translation, and size of the specimens during image acquisition and minimizes the differences between landmark coordinates.

To evaluate variations along latitude and longitude, I created divergence vector scores (DVS) for each specimen and skull angle to summarize combinations of shape variables that contribute the most to shape differences between specimens. DVS were calculated along a variable gradient (latitude and longitude) while controlling for confounding variables (sex, size, and collection year) by using the sums of squares and cross products matrices (SSCP) for the variable of interest. Thus variation produced by

the parameter of interest (e.g, longitude) is exposed while variation attributed to other factors (e.g., sex) is removed (see Appendix S3 for original MANCOVA table). The dimensionality of shape variables was then reduced by a factor analysis to produce the most significant shape variations across the desired gradient. DVS were then used to describe correlations between shape, geographic and environmental variables, and to visualize gradients of shape change (Langerhans, 2009). I used SPSS to generate linear regressions of DVS with geographic and environmental variables. I regressed DVS of latitude and longitude independently over the geographic coordinates of the respective specimen collection localities for each angle. The significance of correlations between shape and geography were evaluated by the *F* statistic, which represents the mean square of the regression divided by the mean square of the residual, and the associated *P* value that tests the null hypothesis of no variation. To evaluate the relationship between climate and shape, the 19 bioclimatic variables downloaded from Worldclim were extracted to the specimen localities using ArcGIS, and principal components were calculated in Rstudio package (available at: http://www.rstudio.com/). I created DVS using the same methods described above, substituting latitude and longitude for the first two principal component (PC) axes, and regressed the scores over the respective PC scores for each skull angle. The significance of these correlations was also evaluated by the *F* statistic and associated *P* value.

I visualized variations in shape with tps Regression version 1.40 (tpsReg; Rolf, 2004; available at: http://life.bio.sunysb.edu/morph/) using divergence vector scores and the corresponding independent variable (latitude, longitude, and the first two PC axes) for each skull angle. Additionally, I generated individual correlations with environmental

variables and geographic variables (latitude and longitude) to determine the aspects of climate that contribute most along geographic gradients.

To evaluate geographic variations in skull size, I calculated centroid size using tpsRelw, representing the square root of the summed squared distances from the landmarks to the average of all the landmark coordinates (the geometric center of the skull; Zelditch, 2004). I then averaged the centroid values between skull angles of the same specimens and regressed them over latitude and longitude in SPSS. The significance was evaluated with the *F* statistic and *P* value. The locations of extremes in centroid size for each skull angle were evaluated in ArcGIS.

RESULTS

1. **Historical and contemporary climatic distribution predictions**:

Model evaluation

All GARP models were statistically significant when evaluated against the null hypothesis and Maxent models performed better than random (AUC = 0.5). Testing ROC AUC for Maxent models ranged from 0.79 – 0.85 for the east and 0.74 – 0.75 for the west models. When evaluated at the 10^{th} percentile of training data, test omission rates ranged from 0.12 – 0.17 for east and 0.13 – 0.15 for the west models. The z-score of partial AUC for testing data was calculated for the GARP models and ranged from $z < 0.001 – 0.03$ for the east and $z < 0.001 – 0.02$ for the west, showing statistical significance. Test omission rates were between 0.09 – 0.13 and 0.09 – 0.12 respectively.

Last Glacial Maximum climatic refugia

The locations of assumed refugia in the northwest and southeast regions of the U.S. were predicted as suitable by all four models respective of the population modeled

(west refugia located in northwest and east refugia located in the southeast). In LGM climate all four western models estimated highly suitable conditions surrounding the southeast and northwest regions of the U.S. and decreased levels of suitability in the Great Plains ecoregion. Additionally, glaciers extending through the Cascade mountain range in the western U.S. may have created a physical barrier to dispersal of refugia (Fig. 2(a) - Maxent, Fig. 3(a) – GARP; Ehlers and Gibbard, 2007; Reding et al., 2012). Suitability predictions under LGM climate for the east population were generally reduced in a latitudinal direction and were significantly decreased in the west. The northern portion of the western Great Plains was also predicted as less suitable for this population. Decreased predictions of suitability in northern Mississippi, Alabama, and Georgia, may be the result of fewer training sampling localities in this region (Fig. 2(b) – Maxent, Fig. 3(b) - GARP). The average percent overlap between east and west estimations of suitable climate was 23.5 for Maxent models and 41.1 for GARP. A combination of elevation, precipitation, and temperature were identified through Maxent MoD analysis to be very different between training (east or west) and projection (North America) regions for climate conditions of the LGM.

Estimated contemporary population distribution

Estimations of suitability for all models in current climate conditions (1950 - 2000) were considerably lower in the Great Plains ecoregion. Models generated for the west population, using four variable sets, identified suitable areas distributions in the eastern and western U.S. and less suitable conditions in Mexico (Fig. 4(b) – Maxent, Fig. 5(b) - GARP). Eastern models predicted the eastern U.S. as highly suitable, for both GARP and Maxent models with the exception of northern Mississippi, Alabama,

Georgia, Tennessee, Kentucky, and the Carolinas. Similarly to the LGM projections, this is possibly due to few sampling localities in this region used to train models. Eastern models also predicted reduced suitability in the western U.S. and Mexico (Fig. 4(a) – Maxent, Fig. 5(a) - GARP). The average percent overlap between east and west suitability predictions was 20 % for Maxent and 43.7 % for GARP. The most dissimilar variables between the training region and the region of projection were identified through the MoD analysis to be both elevation and precipitation of the warmest quarter.

2. **Variations in *Lynx rufus* skull shape and size**:

Centroid size

Linear regressions of the average of the centroid sizes for the skull angles were significant across a latitudinal gradient ($F = 12.153$, $P < 0.001$, $R^2 = 0.053$, $df = 217$; Fig. 6). The largest individual was located on the northern Michigan peninsula and the smallest was sampled from Chihuahua, Mexico.

Latitudinal shape variation

Variations in shape of the VC were significant for DVS along a latitudinal gradient ($F = 20.731$, $P< 0.001$, $R^2 = 0.088$, $df = 217$; Fig. 7(a)). The dominant variations in shape with decreasing latitudes were posterior movement of the maxilla, premaxilla, and palatine regions, lateral compression of the rostrum and expansion of the braincase, and anterior as well as lateral expansion of the zygomatics (Fig. 7(b1)). DVS of the LC were also significantly correlated with latitude ($F = 37.922$, $P< 0.001$, $R^2 = 0.149$, $df = 217$; Fig. 7(a)). Shape changes from north to south included posterior movement of the nasals and premaxilla, and anterior movement of the zygomatic and post orbital process, effectively compressing the rostrum in an anteroposterior direction. Ventral movement of

the lacrimal and infraorbital foramen coupled with dorsal movement of the premaxilla and incisors also suggested dorsoventral compression of the rostrum. However, the dominant movement of the landmarks surrounding the braincase was away from the center with the exception of the occipital condyle which moved dorsally (Fig. 7(b2)). Correlations of shape of the LM were also significant with latitude ($F = 53.014$, $P < 0.001$, $R^2 = 0.197$, df = 217; Fig. 7(a)). Shape changes with decreasing latitude were dominated by dorsoventral expansion of the body of the dentary, anterioposterior increase in the region between the incisors and foramen (the sutured region), and an apparent increase in surface area for muscle attachment of the masseter and temporalis muscles on the coronoid process (Fig. 7(b3)). The DVS were also plotted in geographic space using ArcGIS to show patterns of shape change across latitude (Appendix S4).

Longitudinal shape variation

Regressions of DVS and longitude were significant for the VC ($F = 24.066$, $P<0.001$, $R^2 = 0.100$, df = 217; Fig. 8(a)). The transformation grids showed that the dominant variations in shape from east to west extremes were anterior movement of the rostrum, maxilla, premaxilla, and palatine regions, and oblique lateral and posterior movement toward the midpoint of the braincase for the zygomatics and posterior portions of the cranium, suggesting longer rostrum and smaller braincase in the west (Fig. 8(b1)). A longitudinal gradient was also significantly correlated with shape change in the LC ($F = 93.093$, $P< 0.001$, $R^2 = 0.300$, df = 217; Fig. 8(a)). From east to west, variations showed both dorsal and anterior movement of the rostrum in relation to the orbit. The zygomatic also extended anteriorly and dorsally while the post orbital process extended ventrally (although expansion of the post orbital process may simply reflect individual variation

rather than population variation; Fig. 8(b2)). The braincase was compressed in a dorsoventral direction. Variation in shape of the LM were also significant with longitude ($F = 36.148$, $P < 0.001$, $R^2 = 0.143$, $df = 217$; Fig. 8(a)). The changes with decreasing longitude were dominated by ventral motion of the angular process and mandibular condyle and dorsal motion of the coronoid process (Fig. 8(b3)). Geographic patterns of DVS were also mapped in ArcGIS (Appendix S4).

Environmental correlates

Correlations of environmental variables with latitude and longitude showed that the mean temperature of the coldest quarter varies the most with changes in latitude ($F = 362.39$, $P < 0.001$, $R^2 = 0.591$, $df = 19$) followed by annual mean temperature and the minimum temperature of the coldest month, all representing variations in temperature. Precipitation of the warmest quarter was most highly correlated with longitude ($F = 604.27$, $P < 0.001$, $R^2 = 0.707$, $df = 19$) followed by precipitation of the driest month and temperature annual range.

The first two principal components of the 19 Worldclim bioclimatic variables accounted for 64 % of the climatic variation at the specimen localities. The minimum temperature of the coldest month and temperature annual range contributed most to PC 1 whereas precipitation of the driest quarter and maximum temperature of the warmest month contributed most to PC 2. Shape variations of the VC were significant across the first two principal components (PC 1: $F = 6.013$, $P < 0.05$, $R^2 = 0.027$, $df = 217$; Fig. 9(a); PC 2: $F = 29.000$, $P < 0.001$, $R^2 = 0.0.118$, $df = 217$; Fig. 10(a)). Variations along the PC 1 axis were dominated by slight rostral elongation, anterior movement of the zygomatics, and anteroposterior and lateral compression of the braincase (Fig. 9(b1)). Similarly, along

the PC 2 axis, landmark analyses showed anterior shortening of rostrum, as well as lateral contraction of the palatine and braincase compression in all directions (Fig. 10(b1)). Regressions with DVS of the LC were also significantly correlated with the first two PC axes (PC1: $F = 31.311$, $P < 0.001$, $R^2 = 0.127$, $df = 217$; Fig. 9(a); PC 2: $F = 56.866$, $P < 0.001$, $R^2 = 0.208$, $df = 217$; Fig. 10(a)). There was little variation in the rostral region but visualizations showed compression in the dorsal anterior directions of the temporal process of the zygomatic and dorsoventral compression of the landmarks surrounding the braincase along the PC 1 axis (Fig. 9(b2)). The PC 2 correlations were dominated by ventral movement of the orbit and dorsal motion of the rostrum. There was anterior motion of the zygomatic in addition to the post orbital process and the landmarks surrounding the braincase suggested anteroposterior expansion and slight ventral compression (Fig. 10(b2)). Shape changes of the LM were also significant along the first two PC axes (PC 1: $F = 17.726$, $P < 0.001$, $R^2 = 0.076$, $df = 217$; Fig. 9(a); PC 2: $F = 32.364$, $P < 0.001$, $R^2 = 0.130$, $df = 217$; Fig. 10(a)). Along the PC 1 axis, vectors showed a possible increase in height of the coronoid process (Fig. 9(b3)). On the PC 2 axis, variation in the lateral mandible was dominated by expansion in both height and width of the coronoid process and ventral motion of the angular process and mandibular condyle (Fig. 10(b3)).

DISCUSSION

Ecology and morphology as predictors of geographic distance and population identity

My ecological niche models supported the hypothesis that the longitudinal genetic cline between eastern and western populations of *L. rufus* corresponds with the climate and geography of the central Great Plains ecozone. Although genetic data shows that

some long–distance migrants do disperse across the Great Plains (Reding et al., 2012) and suitable conditions exist on either side of this barrier, the contemporarily dominant grassland and row crop agriculture in this region, shown to be avoided by this species (Tucker et al. 2008; Reding et al., 2012), coupled with the bobcat's preference for understory vegetation may be restricting higher levels of migration and gene flow, effectively maintaining the genetic subdivision discovered by Reding et al. (2012). Although my study did not take into consideration specifically these land cover types, the bioclimatic variables evaluated and morphology together may account for the abiotic and biotic variables that are representative of habitat types (e. g., Soberón and Martínez-Gordillo, 2012). The two concentrations of ancestral haplotypes shown by the mtDNA structure of *L. rufus,* one clustered along the west coast of the U.S. and the other in the southeast, exhibited rapid expansion from these geographic origins corresponding to glacial recession and within approximately the last 10 ka (Reding et al., 2012). During historical climate cycles the glacial barriers in high elevation regions may have acted as physical obstacles, preventing the expansion of these populations (Reding et al., 2012). A broad–scale genetic analysis of the grey wolf (*Canis lupus*) revealed a similar scenario (Vila et al., 1999), however with multiple range contractions and expansions of fragmented populations in association with the cycles of glaciers during the Pleistocene epoch. Interglacial periods allowed mixing of populations, resulting in reduced genetic variability across the range of grey wolves contemporarily. If ephemeral glaciers were the only boundary historically preventing gene flow among populations of *L. rufus*, a similar pattern should emerge. Their genetically disparate populations instead suggest that a more enduring obstacle to dispersal is present (Reding et al., 2012). A similar situation

exists in Painted Buntings (*Passerina ciris*), with a contemporary and persistent barrier to breeding populations likely stemming from LGM isolation into eastern and western refugia (Shipley et al., 2013). When current ENMs were projected onto the LGM climate dataset, suitability was reduced in a latitudinal direction and decreased suitability in the central U.S. remained apparent, feasibly creating refugia for the extent of advanced glaciation. The present models did not depict climatic constraints necessarily consistent with aridification of the Great Plains during historical climate as a more enduring obstacle, as suggested by Remington (1968). The however did show that elevation, particularly the Rocky Mountains, may be a contributing factor in reducing migration. Suitability conditions were significantly reduced across the continental divide for several of the models, in addition to reduced levels through the Great Plains during contemporary climate, possibly corresponding to the rain shadow effect generated by the Rocky Mountains and present in both climate datasets (present and LGM). Fossil evidence further supports the existence of a persisting genetic barrier. Thus far, *L. rufus* specimens have been absent from the Great Plains for the duration of the Pleistocene epoch (35-10 ka), but can be found in areas surrounding this region and were more widespread geographically prior to the Pleistocene (Graham and Lundelius, 2010).

Geometric morphometric analyses also revealed strong correlations of shape with geographic and environmental variables. Linear trends across a longitudinal gradient suggested significant shape variation across their geographic range, however these analyses did not reflect a longitudinal cline. Visualizations of the extreme shapes in tpsRegr supported the hypothesis of isolation in the northwest and southeast portions of the U.S. Similar morphologies occurring in the south and east (generally shorter and

broader skulls) and in the north and west (generally longer and thinner skulls) suggest that these morphologies may have originated in the locations of ancestral refugia. Despite this support for refugia, an indistinct cline between the morphologies of the east and west populations is more representative of an isolation by distance pattern or may suggest that environmental variation plays a significant role in the phenotype of this species.

Ecological and functional implications for variations in skull shape

Bergmann's rule certainly holds true for this mammalian species (Blackburn et al., 1999). Northern individuals are on average larger than their southern counterparts, with specimens collected from northern Michigan among the largest of all specimens used in this study. This is also in accordance with selection of prey. Individuals in the north are more likely to prey on larger animals such as white–tailed deer (*Odocoileus virginianus;* Toweill Anthony, 1988; Story et al., 1982; Litvaitis et al., 1984; Litvaitis et al. 1987; Matlack and Evans, 1992), as opposed to the south where a larger proportion of smaller mammals, reptiles, and birds are taken as prey (Fritts and Sealander, 1978; Maehr and Brady, 1986). Deer are also taken in the south on occasion (Gashwiler et al., 1960), more frequently in winter months when smaller rodents may be more scarce (Maehr and Brady, 1986); the proportion of scavenging compared with killing of larger animals however is difficult to determine (Platt et al., 2010). Badgley and Fox (2000) concluded that in addition to a positive relationship between size and latitude, size of species also generally increases from east to west, however my centroid size analysis does not show this relationship to be significant for bobcats.

Skull morphology and the feeding apparatus are highly sensitive to external environmental variations and can likely be considered a representation of biotic

influences (e. g., Soberón and Martínez-Gordillo, 2012). Bobcats are primarily solitary, ambush predators that, like most felids, kill with a single bite to a vital region of the body such as the neck (Slater et al. 2009). Thus, muscle size, bite force, and bite size (gape) are all related to the diet of the bobcat. Gape is possibly the most important factor in determining what size prey an animal can eat. To provide a lethal bite, the prey must fit between the upper and lower canines. Two ways gape can be increased are by elongation of the rostrum and ventrally displacing the articulation of the jaw to increase the maximum rotation (Slater et al., 2009). Our study showed that bobcats in both northern and western regions of the their range exhibited rostral elongation, with additional ventral displacement of the mandibular condyle apparent in the LM of the western individuals, providing a large bite size for preying on larger mammals. Additionally, a larger gape also allows for more diversity in diet. The geologically unstable and topographically diverse landscape of western North America has provided for intense speciation compared with the east, resulting in higher species diversity (Badgley et al., 2000). Increased diversity in diet selection in western bobcats is also evident by diet analyses (e. g., Toweill and Anthony, 1988). An increase in the diversity of species and the diet of bobcats also occurs latitudinally, toward the equator, likely due to temperature increases (Rohde, 1992; Delibes et al., 1997), this however was not clear in the present large scale morphological analysis. We speculate that the opportunistic nature of bobcats is reflected in their diet. The occupation of a great latitudinal gradient in the western portion of their range may explain the increase in prey diversity at lower longitudes. Ventral displacement on the jaw joint and expansion of the coronoid process exhibited in southern individuals is likely associated with increases in species diversity toward the

south. The development of shorter versus longer rostrums and associated gape size during isolation is likely a reflection of prey size rather than diversity in the locations of assumed LGM refugia. Shape analyses at small scales, taking into account regional climate and habitat variations, may show additional pockets of local adaptation in the cranium and mandible of this species as is suggested by diet differences across landscape types within North America (e. g., Fritts and Sealander, 1978). Slater and Van Valkenburgh (2009) suggested that there is a trade–off between gape size and bite force, leverage, and efficiency; however, additional leverage may be attained by increasing the length of the coronoid process. The latter hypothesis is supported by the present LM analyses of the western population. Slater and Van Valkenburgh (2009), among others, additionally conclude that musculature and bite force is generally scaled positively with allometry and jaw length by analyses of muscle cross–sectional area, muscle mass, fiber length, and force (e. g., Hartstone – Rose et al., 2012). I expect that further functional analyses of musculature and bone thickness would provide evidence of a proportional increase in bite force of bobcats with elongated rostrums in the northern and western portion of their range.

Significant correlations with the principle components of climate revealed that variations in precipitation (most influenced by longitude) and temperature (highly influenced by latitude) are certainly relevant in the morphological diversity of this species. It is particularly interesting to find that precipitation of the warmest quarter of the year was the highest correlated variable with longitudinal variation, additionally found by Reding et al. (2012) to make the largest climatic contribution to the spatial organization of bobcat genetic structure. Shape variations across the first principal

component, dominated by temperature, were similar to morphological variations that occurred along a latitudinal gradient, supporting temperature as the dominant climatic factor influencing changes with latitude and thus variations in prey availability. The more complicated morphological variations that occurred with the second principal component may be attributed to variations in both precipitation and temperature and thus do not directly reflect variation similar to that across one geographic gradient, particularly if a genetic component is contributing to an east to west divergence in shapes.

CONCLUSIONS

Climate models support the genetic assessment for distinct east and west populations of *L. rufus* having diverged from refugia isolated in the northwest and southeast regions of the U.S. during LGM climate (Reding et al., 2012). The present models also suggested a zone of secondary contact may be present in the central Great Plains ecoregion, supporting theories of a suture zone in this region (Remington, 1968). Ecological results of this study additionally suggest that the Rocky Mountains and the reduction in rainfall along their eastern border may be contributing to low levels of gene flow between these populations. Morphological analyses however, suggest that the skeletal phenotype of bobcats does not closely resemble a genetic east, west cline. Instead, morphological characteristics from east to west are likely the result of more complex associations with environmental characteristics. However, the story of bobcat evolution in light of climatic and morphological characters is much more complex than this study alone can convey. Both seasonal changes and sexual dimorphism also play a major role in the diet and thus morphology of individuals and populations of *L. rufus*. Diet and morphological studies have suggested that not only does prey selection change

significantly by season (in association with prey availability), but that it also varies between sexes, particularly in high altitudes and latitudes (Sikes and Kennedy, 1992; Dobson et al., 1996). Riley (1999) stated that in the far northern portion of their range, male and female bobcats are so distinct from one another in size that they appear to be entirely different species. Such a large disparity in size between sexes gives further support for prey partitioning, with deer making up a larger portion of the diet of males than females as described by diet analyses (Toweill and Anthony, 1988; Mclean et al., 2005). Additionally, sympatric occupancy of regions with other carnivores such as the puma or coyote may cause further partitioning of prey when smaller scale studies are conducted (Maehr and Brady, 1986). Further research on morphological divergence due to sexual dimorphism, prey partitioning, and variations in season and climate would increase our comprehension of the role of climate and ecology on the complex history of this species.

REFERENCES

Badgley, C. & Fox, D.L. (2000) Ecological Biogeography of North American Mammals: Species Density and Ecological Structure in Relation to Environmental Gradients. *Journal of Biogeography*, 27, 1437-1467.

Blackburn, T.M., Gaston, K.J. & Loder, N. (1999) Geographic gradients in body size: a clarification of Bergmann's rule. *Diversity and Distributions*, 5, 165-174.

Braconnot, P., Harrison, S.P., Joussaume, S., Hewitt, C.D., Kitoh, A., Kutzbach, J.E., Liu, Z., Otto-Bliesner, B., Syktus, J. & Weber, N. (2004) Evaluation of PMIP coupled ocean-atmosphere simulations of the mid-Holocene. *Past Climate Variability through Europe and Africa* (ed. by R.W. Batterbee, F. Gassee, and C.E. Stickley), pp. 515-533. Springer Netherlands, New York.

Chamberlain, M.J., Leopold, B.D. & Conner L.M. (2003) Space use, movements and habitat selection of adult bobcats (Lynx rufus) in central Mississippi. *American Midland Naturalist*, 149, 395-405.

Commission for Environmental Cooperation. (1997) *Ecological Regions of North America: Toward a Common Perspective*. CEC, Montreal. Available at: <http://www.cec.org> (Accessed 12 January 2014).

Davis, J.M. & Stamps, J.A. (2004) The effects of natal experience on habitat preferences. *Trends in Ecology and Evolution*, 19, 411-416.

Delibes, M., Blázquez, M.C., Rodriguez-Estrella, R. & Zapata, S.C. (1997) Seasonal food habits of bobcats (*Lynx rufus*) in subtropical Baja California Sur, Mexico. *Canadian Journal of Zoology*, 74, 478-483.

Dobson, F.S., Wigginton, J.D. (1996) Environmental influences on the sexual dimorphism in body size of wetern bobcats. *Oecologia*, 108,610-616.

Dormann, C.G., Elith, J., Bacher, S., Buchmann, C., Carl, G., Carré, G., García Marquéz, J.R., Gruber, B., Lafourcade, B., Leitão, P.J., Münkemüller, T., McClean, C., Osborne, P.E., Reineking, B., Shröder, B., Skidmore, A.K., Zurell, D. & Lautenback, S. (2012) Collinearity: a review of methods to deal with it and a simulation study evaluating their performance. *Ecography*, 35, 001-020.

Ehlers, J. & Gibbard, P.L. (2007) The extent and chronology of Cenozoic Global Glaciation. *Quaternary International*, 164-165, 6-20.

Elbroch, M. (2006) Animal Skulls: a guide to North American species. Stackpole Books, Mechanicsburg, PA.

Evin, A., Horacek, I. & Hulva, P. (2011) Phenotypic diversification and island evolution of pipistrelle bats (Pipistrellus pipistrellus group) in the Mediterranean region inferred from geometric morphometrics and molecular phylogenetics. *Journal of Biogeography*, 38, 2091-2105.

Fritts, S.H. & Sealander, J.A. (1978) Diets of Bobcats in Arkansas with Special Reference to Age and Sex Differences. *The Journal of Wildlife Management,* 42, 533-539.

Fox, L.B. (1990) *Ecology and population biology of the bobcat, Felis rufus in New York.* Doctoral Dissertation (Abstract), State University of New York, College of Environmental Science and Forestry, Syracuse, New York, USA.

Fitzpatrick, B.M. & Turelli, M. (2006) The geography of mammalian speciation: mixed signals from phylogenies and range maps. *Evolution*, 60, 601-615.

Garcia-Perea, R (1996) Patterns of postnatal development in skulls of Lynxes, genus Lynx (Mammalia: Carnivora). *Journal of Morphology*, 229, 241-254.

Graham, R.W. & Lundelius Jr., E.L. (2010) FAUNMAP II: new data for North America with a temporal extension for the Blancan, Irvingtonian and early Rancholabrean. FAUNMAP II Database, version 1.0. Available at: <http://www.ucmp.berkeley.edu/faunmap> (accessed 3 May 2013).

Gashwiler, J.S., Robinette, W.L., & Morris, O.W. (1960) Food of bobcats in Utah and eastern Nevada. *Journal of Wildflife Management*, 24, 226-229.

Haag, T., Santos, A.S., Sana, D.A., Morato, R.G., Cullen, Jr.L., Crawshaw, Jr.P.G., De Angelo, C., Di Bitetti, M.S., Salzano, F.M. & Eizirik, E. (2010) The effect of habitat fragmentation on the genetic structure of a top predator: loss of diversity and high differentiation among remnant populations of Atlantic Forest jaguars (Panthera onca). *Molecular Ecology*, 19, 4906-4921.

Hansen, K. (2007). Bobcat master of survival. Oxford University Press, Inc., New York.

Harrison, S.P., Braconnot, P., Joussaume, S., Hewitt, C.D. & Stouffer, R.J. (2002) Comparison of paleoclimate simulations enhances confidence in models. *Eos, Transactions American Geophysical Union*, 83, 447.

Hartstone-Rose, A., Perry, J.M. & Morrow, C.J. (2012) Bite Force Estimation and the Fiber Architecture of Felid Masticatory Muscles. *The Anatomical Record*, 295, 1336-1351.

Hass, C.C. (2009) Competition and coexistence in sympatric bobcats and pumas. *Journal of Zoology*, 278, 174-180.

Hijmans, R.J., Cameron, S.E., Parra, J.L., Jones, P.G. & Jarvis, A. (2005) Very high resolution interpolated climate surfaces for global land areas. *International Journal of Climatology*, 25, 1965-1978.

Jimenez-Valverde, A. (2012) Insights into the area under the receiver operating characteristic curve (AUC) as a discrimination measure in species distribution modelling. *Global Ecology and Biogeography*, 21, 498-507.

Kapfer, P.M. & Potts, K.B. (2012) Socioeconomic and ecological correlates of bobcat harvest in Minnesota. *Journal of Wildlife Management*, 76, 237-242.

Klingenberg, C.P. (2011) MorphoJ: an integrated software package for geometric morphometrics. *Molecular Ecology Resources*, 11, 353-357. Available at: <www.flywings.org.uk/MorphoJ_page.htm> (accessed 13 April 2013).

Kozak, K.H., Graham, C.H., & Wiens, J.J. (2008) Integrating GIS-based environmental data into evolutionary biology. *Trends in Ecology and Evolution*, 23, 141-148.

Langerhans, R.B. (2009) Trade – off between steady and unsteady swimming underlies predator – driven divergence in *Gambusia affinis*. *Journal of Evolutionary Biology*, 22, 1057-1075.

Latch, E.K., Reding, D.M., Heffelfinger, J.R., Alcalá-Galván, C.H. & Rhodes, Jr., O.E. (2014) Range – wide analysis of genetic structure in a widespread, highly mobile species (*Odocoileus hemionus*) reveals the importance of historical biogeography. *Molecular Ecology*, 23, 3171-3190.

Licht, D.S. (2010) Observations of bobcats, *Lynx rufus*, hunting black-tailed prairie dogs, *Cynomys ludovicianus,* in western South Dakota. *Canadian Field-Naturalist*, 124, 209-214.

Litvaitis, J.A., Major, J.T. & Sherburne, J.A. (1987) Influence of season and human-induced mortality on spatial-organization of bobcats (*Felis rufus*) in Maine. *Journal of Mammalogy*, 68, 100-106.

Litvaitis, J.A., Stevens, C.L. & Mautz, W.W. (1984) Age, Sex, and Weight of Bobcats in Relation to Winter Diet. *The Journal of Wildlife Management*, 48, 632-635.

Maehr, D.S., & Brady, J.R. (1986) Food habits of bobcats in Florida. *Journal of Mammalogy*, 67, 133-138.

Marcus, L.F., Hingst-Zaher, E. & Zaher, H. (2000) Application of landmark morphometrics to skulls representing the orders of living mammals. *Hystix the Italian Journal of Mammology*, 11, 27-47.

Matlack, C.R. & Evans, A.J. (1992) Diet and condition of bobcats, *Lynx rufus*, in Nova Scotia during autumn and winter. *Canadian Journal of Zoology*, 70, 1114-1119.

Mattern, M.Y. & McLennan, D.A. (2000) Phylogeny and speciation of felids. *Cladistics*, 16, 232-253.

McLean, M.L., McCay, T.S. & Lovallo, M.J. (2005) Influences of Age, Sex and Time of Year on Diet of the Bobcat (Lynx rufus) in Pennsylvania. *American Midland Naturalist*, 153, 450-453.

Millions D.G. & Swanson, B.J. (2007) Impact of natural and artificial barriers to dispersal on the population structure of bobcats. *The Journal of Wildlife Management*, 71, 96-102.

Patterson, B.D., Ceballos, G., Sechrest, W., Tognelli, M.F., Brooks, T., Luna, L., Ortega, P., Salazar, I. & Young, B.E. (2003) Digital distribution maps of the mammals of the western hemisphere, version 1.0. NatureServe, Arlington, Virginia, USA.

Phillips S.J. & Dudik M. (2008) Modeling of species distributions with Maxent: new extensions and a comprehensive evaluation. *Ecography*, 31, 161-175.

Pilot M., Jedrzejewski W., Branicki W., Sidorovich V.E., Jedrzejewska B., Stachura K. & Funk S.M. (2006) Ecological factors influence population genetic structure of European grey wolves. *Molecular Ecology*, 15, 4533-4553.

Platt, S.G., Salmon, G.T., Miller, S.M. & Rainwater, T.R. (2010) Scavenging by a Bobcat, *Lynx rufus*. *Canadian Field-Naturalist*, 124, 265-267.

Reding, D. M., Bronikowski, A.M., Johnson, W.E. & Clark, W.R. (2012) Pleistocene and ecological effects on continental-scale genetic differentiation in the bobcat (*Lynx rufus*). *Molecular Ecology*, 21, 3078-3093.

Remington, C.L. (1968) Suture-zones of hybrid interaction between recently joined biotas. *Evolutionary Biology*, 2, 321-428.

Riley, S.P.D. (1999) *Spatial organization, food habits and disease ecology of bobcats (Lynx rufus) and gray foxes (Urocyon cinereoargenteus) in national park areas in urban and rural Marin County, California (Golden Gate National Recreation Area)*. Doctoral dissertation, University of California, Davis, CA. (Abstract)

Rohde, K. (1992) Latitudinal gradients in species diversity: the search for the primary cause. *Oikos*, 65,514-527.
Rohlf, F.J. & Slice, D. (1990) Extensions of the Procrustes Method for the Optimal Superimposition of Landmarks. *Systematic Zoology*, 39, 40-59.
Rohlf, F.J. (2004) tps series softwares. Available at: <http//life..bio.sunysb.edu/morph/>.
Rolley, R.E. (1983) *Behavior and population dynamics of bobcats in Oklahoma*. Doctoral Dissertation (Abstract), Oklahoma State University, Stillwater, Oklahoma, USA.
Rueness, E.K., Stenseth, N.C., O'Donoghue, M., Boutin, S., Ellegren, H. & Jakobsen, K.S. (2003) Ecological and genetic spatial structuring in the Canadian lynx. *Letters to Nature*, 425, 69-72.
Sacks B.N., Brown S.K. & Ernest H.B. (2004) Population structure of California coyotes corresponds to habitat-specific breaks and illuminates species history. *Molecular Ecology*, 13, 1265-1275.
Schliewen, U.K., Tautz, D. & Paabo, S. (1994) Sympatric speciation suggested by monophyly of crater lake cichlids. *Nature*, 368, 629-632.
Schmidly, D.J. & Read, J.A. (1986) Cranial variations in the bobcat (*Felis rufus*) for Texas and surrounding states. *Occasional Papers the Museum,* Texas and surrounding states. *Occasional Papers the Museum,* Texas Tech University Press. 101, 1-39.
Shipley, J.R., Contina, A., Batbayar, N., Bridge, E.S., Peterson, A.T. & Kelly, J.F. (2013) Niche conservatism and disjunct populations: a case study with painted buntings (*Passerina ciris*). *The Auk*, 130, 476-486.
Sikes, R.S. & Kennedy, M.L. (1992) Morphologic Variation of the Bobcat (Felis-Rufus) in the Eastern United-States and Its Association with Selected Environmental Variables. *American Midland Naturalist*, 128, 313-324.
Slater, G.J. & Van Valkenburgh, B. (2009) Allometry and performance: the evolution of skull form and function in felids. *Journal of Evolutionary Biology*, 22, 2278-2287.
Soberón, J. & Martínez-Gordillo, D. (2012) Occupation of environmental and morphological space: climate niche and skull shape in *Neotoma* woodrats. *Evolutionary Ecology Research*, 14, 503-517.
Soberón, J. & Peterson, A.T. (2005) Interpretation of models of fundamental ecological niches and species' distributional areas. *Biodiversity Informatics,* 2, 1-10.
Story, J.D., Galbraith, W.J. & Kitchings, J.T. (1982) Food Habits of Bobcats in Eastern Tennessee. *Journal of the Tennessee Academy of Science*, 57, 29-32.
Swenson, N.G. & Howard D.J. (2005) Clustering of contact zones, hybrid zones, and phylogeographic breaks in North America. *The American Naturalist*, 166, 581-591.
Tanner, J.B., Zelditch, M.L., Lundrigan, B.L. & Holekamp, K.E. (2010) Ontogenetic change in skull morphology and mechanical advantage in the Spotted Hyena (*Crocuta crocuta*). *Journal of Morphology*, 271, 353-365.
Toweill, D.E. & Anthony, R.G. (1988) Annual diet of bobcats in Oregon's Cascade Range. *Northwest Science*, 62, 99-103.
Tucker, S.A., Clark, W.R. & Gosselink, T.E. (2008) Space use and habitat selection by bobcats in the fragmented landscape of south-central Iowa. *Journal of Wildlife Management*, 72, 1114-1124.

Waltari, E., Hijmans, R.J., Peterson, A.T., Nyári, Á.S., Perkins, S.L. & Guralnick, R.P. (2007) Locating Pleistocene refugia: comparing phylogeographic and ecological niche model predictions. *Plos One*, 2, 1-11.

Werdelin, L. (1983) Morphological Patterns in the Skulls of Cats. *Biological Journal of the Linnean Society*, 19, 375-391.

Western Ecology Division. (2013) Primary distinguishing characteristics of level III ecoregions of the continental United States. *U.S. Environmental Protection Agency*. Available at: <http://www.epa.gov/wed/pages/ecoregions/level_iii_iv.htm>. (Accessed 10 October 2013).

Wigginton, J.D. & Dobson, F.S. (1999) Environmental influences on geographic variation in body size of western bobcats. *Canadian Journal of Zoology-Revue Canadienne De Zoologie*, 77, 802-813.

Wooding, S. & Ward, R. (1997) Phylogeography and Pleistocene evolution in the North American black bear. *Molecular Biology and Evolution*, 14, 1096-1105.

Vila, C., Amorim, I.R., Leonard, J.A., Posada, D., Castroviejo, J., Petrucci-Fonseca, F., Crandall, K.A., Ellegren, H. & Wayne, R.K. (1999) Mitochondrial DNA phylogeography and population history of the grey wolf *Canis lupus*. *Molecular Ecology*, 8, 2089-2103.

Zelditch, M.L., Swiderski, D.L., Sheets, H.D. & Fink, W.L. (2004) Geometric morphometrics for biologists: a primer, 2nd edn. Elsevier Academic Press, London.

TABLES

Table 1. The four variable sets derived from the 19 bioclimatic variables used to generate ecological niche models with Maxent and GARP.

1	2	3	4
Precipitation of the warmest quarter	Precipitation of the warmest quarter	Precipitation of the warmest quarter	Precipitation of the warmest quarter
Mean diurnal range	Mean diurnal range	Mean diurnal range	Mean diurnal range
Mean temperature of the wettest quarter	Mean temperature of the wettest quarter	Mean temperature of the wettest quarter	Mean temperature of the wettest quarter
Altitude	Altitude	Precipitation of the coldest quarter	Altitude
Precipitation of the coldest quarter	Temperature annual range	Annual mean temperature	Temperature annual range
Temperature seasonality	Temperature seasonality		
Mean temperature of the coldest quarter	Precipitation seasonality		

FIGURES

Fig. 1. Geographic localities used to generate east (circles) and west (triangles) ecological niche models overlaying the known geographic range of *Lynx rufus* (range map produced by Nature Serve, Patterson et al., 2003).

Fig. 2. Thresholded consensus predictions of suitability created by Maxent for (a) west and (b) east clades projected onto the climate of the last glacial maximum (21,000 ka) shown with the predicted extent of the Laurentide Glacier (North American glacier; Ehlers and Gibbard, 2007). The degree of suitability is represented as the number of models (0 – 4) that predicted suitability and is shown in a gray scale (darkest – 4 models predicted suitability, etc.; geographic coordinate system is North American 1983).

Fig. 3. Thresholded consensus predictions of suitability created by GARP for (a) west and (b) east clades projected onto the climate of the last glacial maximum (21,000 ka) shown with the predicted extent of the Laurentide Glacier (North American glacier; Ehlers and Gibbard, 2007). The degree of suitability is represented as the number of models (0 – 4) that predicted suitability and is shown in a gray scale (darkest – 4 models predicted suitability, etc.; geographic coordinate system is North American 1983).

Fig. 4. Thresholded consensus predictions of suitability generated by Maxent for (a) east and (b) west genetic populations projected onto current climate conditions. The degree of suitability is represented as the number of models (0 – 4) that predicted suitability and is shown in a gray scale (darkest – 4 models predicted suitability, etc.; geographic coordinate system is North American 1983).

Fig. 5. Thresholded consensus predictions of suitability generated by GARP for (a) east and (b) west genetic populations projected onto current climate conditions. The degree of suitability is represented as the number of models (0 – 4) that predicted suitability and is shown in a gray scale (darkest – 4 models predicted suitability, etc.; geographic coordinate system is North American 1983).

Fig. 6. Linear regressions of centroid size averaged across each skull angle showing a positive correlation with latitude.

Fig. 7. (a) Linear regressions of divergence vector scores (DVS) and latitude for three angles of the skull (lateral cranium and ventral cranium overlay one another) and (b) transformation grids showing shape deviations at each landmark from the mean shape for

(1) ventral cranium, (2) lateral cranium, and (3) lateral mandible along a latitudinal gradient (shown at 10x the observed range).

Fig. 8. (a) Linear regressions of divergence vector scores (DVS) and longitude for three angles of the skull and (b) transformation grids showing shape deviations at each landmark from the mean shape for (1) ventral cranium, (2) lateral cranium, and (3) lateral mandible along a longitudinal gradient (shown at 10x the observed range).

Fig. 9. (a) Linear regressions of divergence vector scores (DVS) and the first principle component (PC1) for three angles of the skull and (b) transformation grids showing shape deviations at each landmark from the mean shape for (1) ventral cranium, (2) lateral cranium, and (3) lateral mandible between the most highly contributing variables along the PC1 axis (shown at 10x the observed range).

Fig. 10. (a) Linear regressions of divergence vector scores (DVS) and the second principle component (PC2) for three angles of the skull and (b) transformation grids showing shape deviations at each landmark from the mean shape for (1) ventral cranium, (2) lateral cranium, and (3) lateral mandible between the most highly contributing variables along the PC2 axis (shown at 10x the observed range).

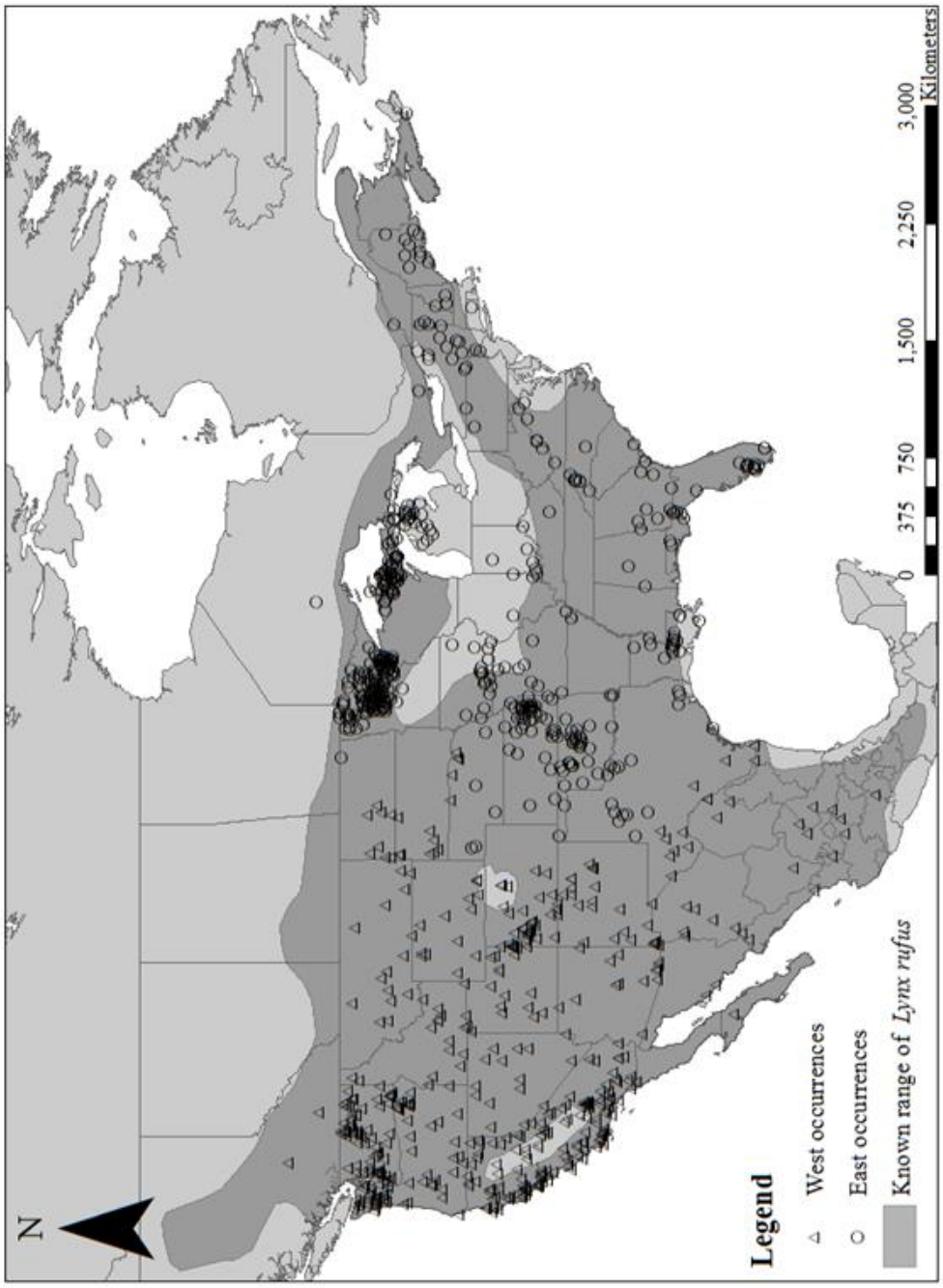
N
Legend
West occurrences
East occurrences
Known range of Lynx rufus
0
375
750
1,500
2,250
3,000
Kilometers

Fig. 1

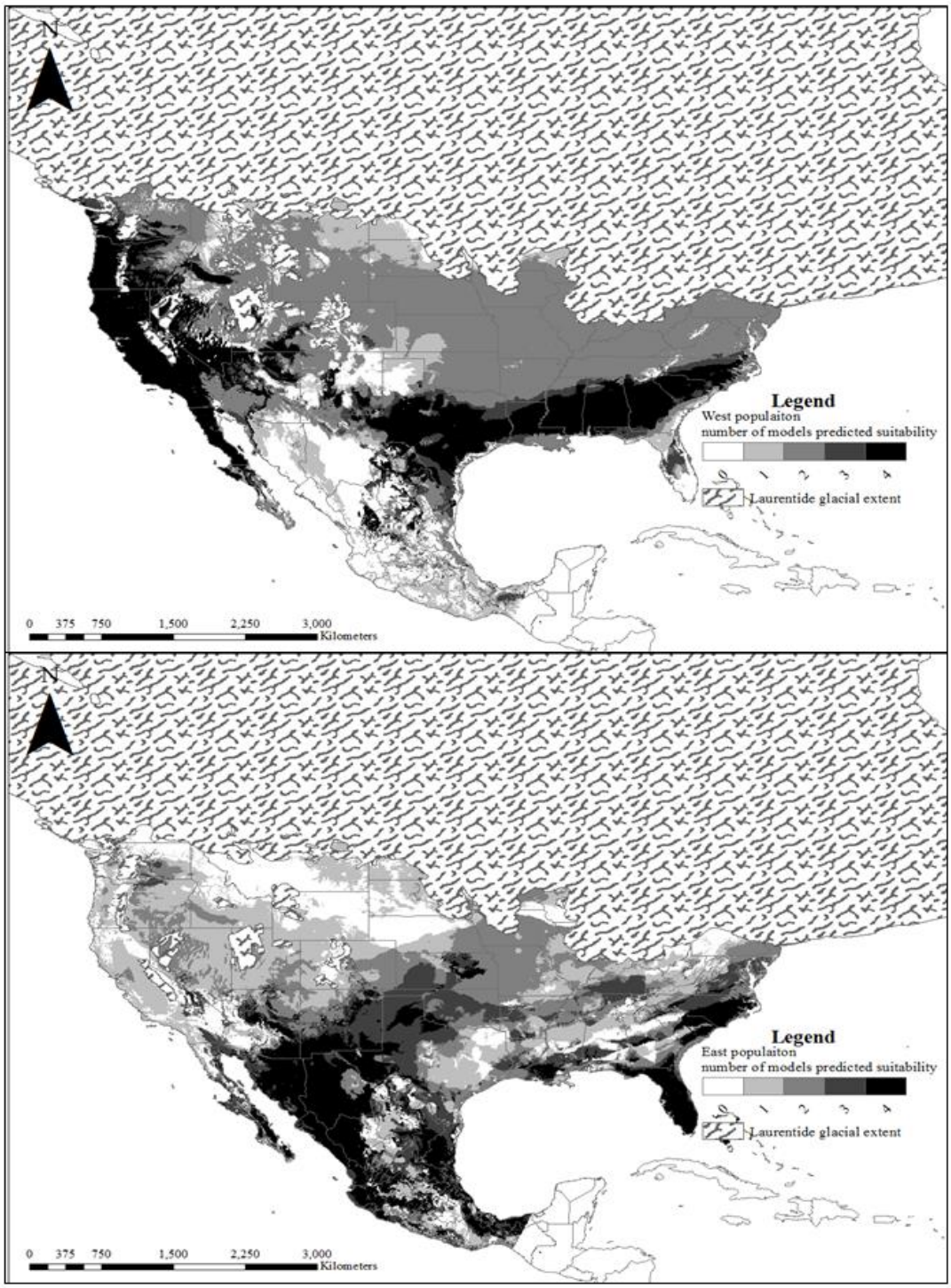
(a)
N
Legend
West populaiton
number of models predicted suitability
0
1
2
3
4
Laurentide glacial extent
0 375 750 1,500 2,250 3,000
Kilometers
(b)
N
Legend
East populaiton
number of models predicted suitability
0
1
2
3
4
Laurentide glacial extent
0 375 750 1,500 2,250 3,000
Kilometers

Fig. 2

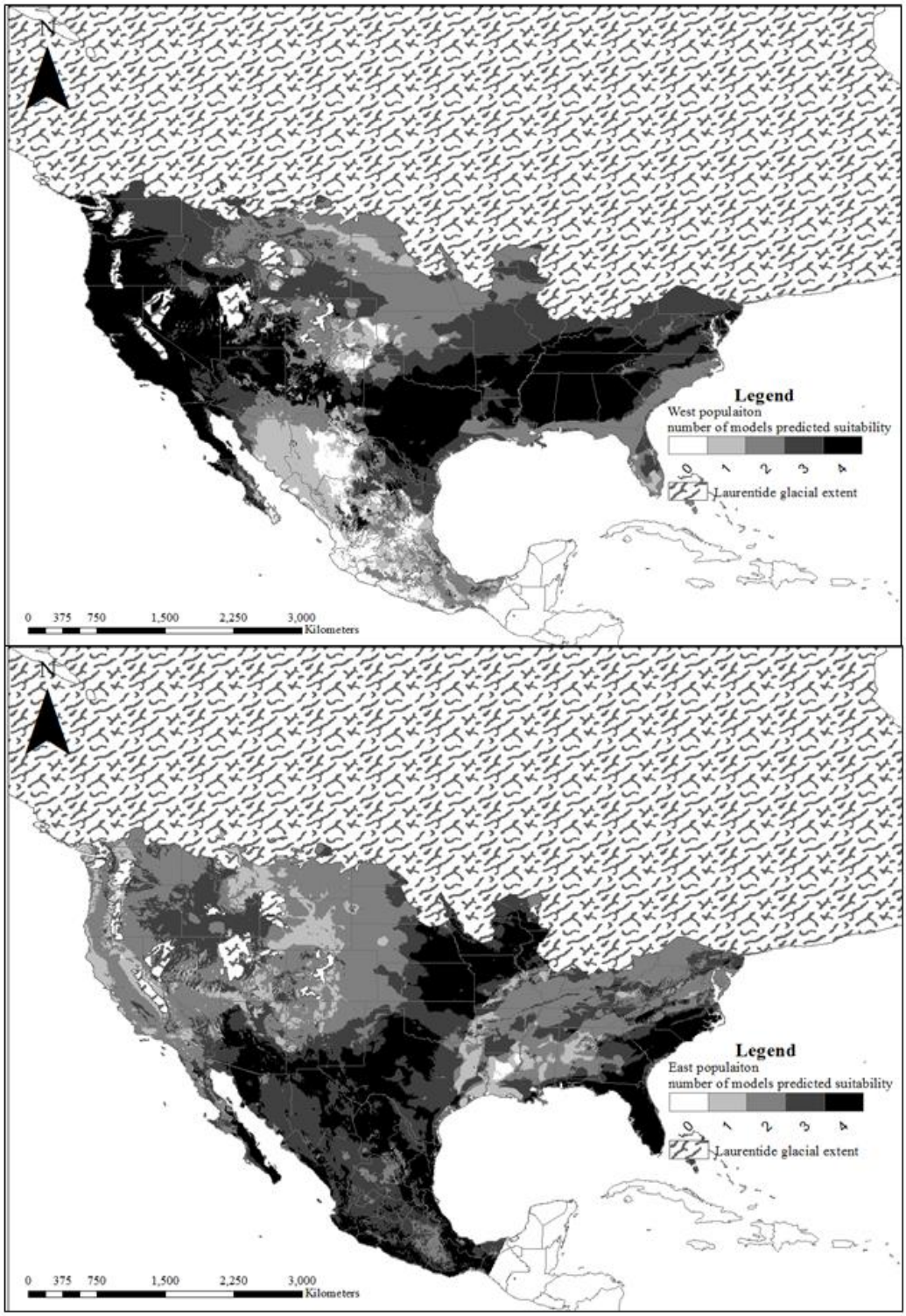
N
Legend
West populaiton
number of models predicted suitability
0 1 2 3 4
Laurentide glacial extent
0 375 750 1,500 2,250 3,000
Kilometers
(a)
N
Legend
East populaiton
number of models predicted suitability
0 1 2 3 4
Laurentide glacial extent
0 375 750 1,500 2,250 3,000
Kilometers
(b)

Fig. 3

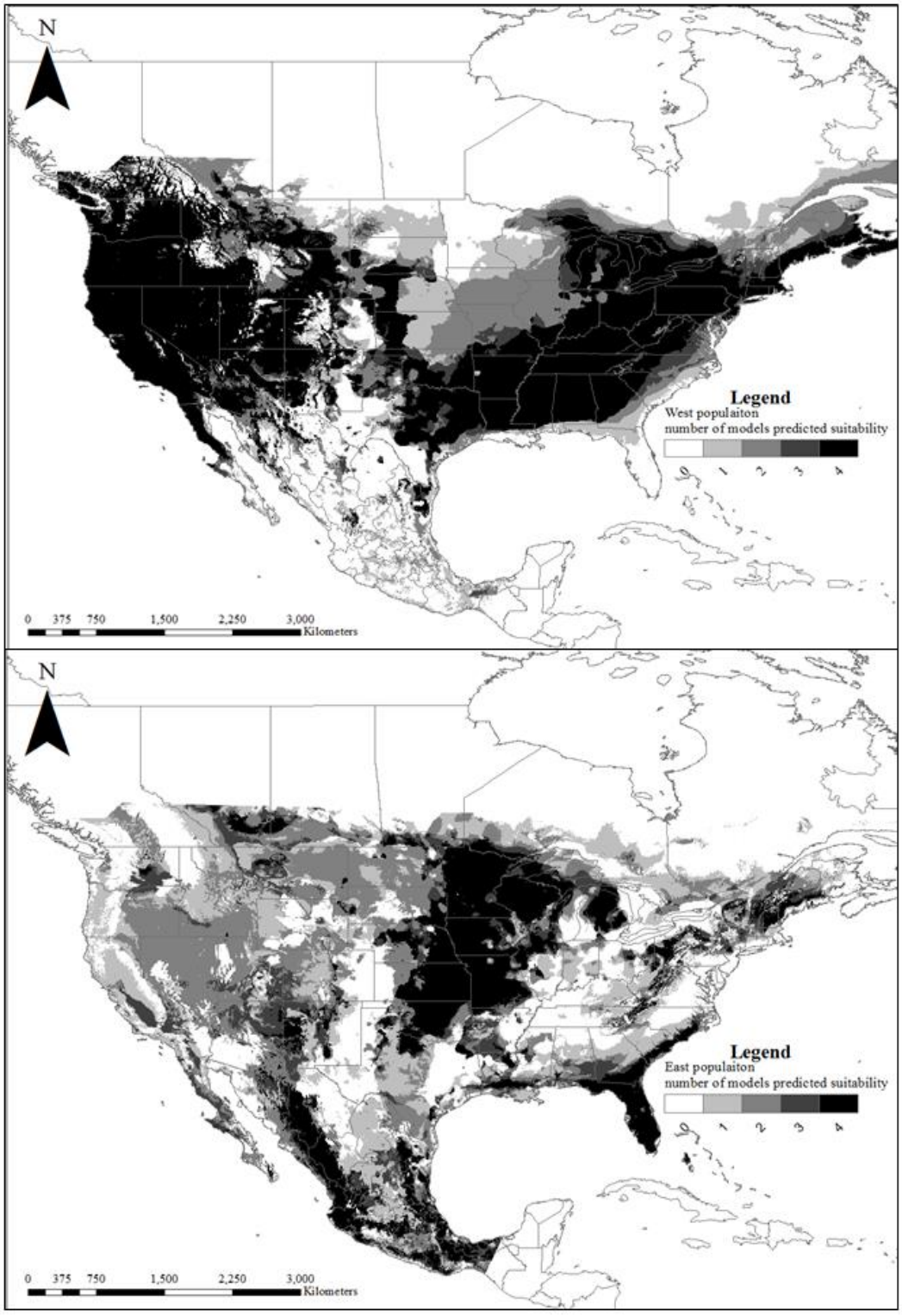
N
Legend
West populaiton
number of models predicted suitability
0 1 2 3 4
0 375 750 1,500 2,250 3,000
Kilometers
(a)
N
Legend
East populaiton
number of models predicted suitability
0 1 2 3 4
0 375 750 1,500 2,250 3,000
Kilometers
(b)

Fig. 4

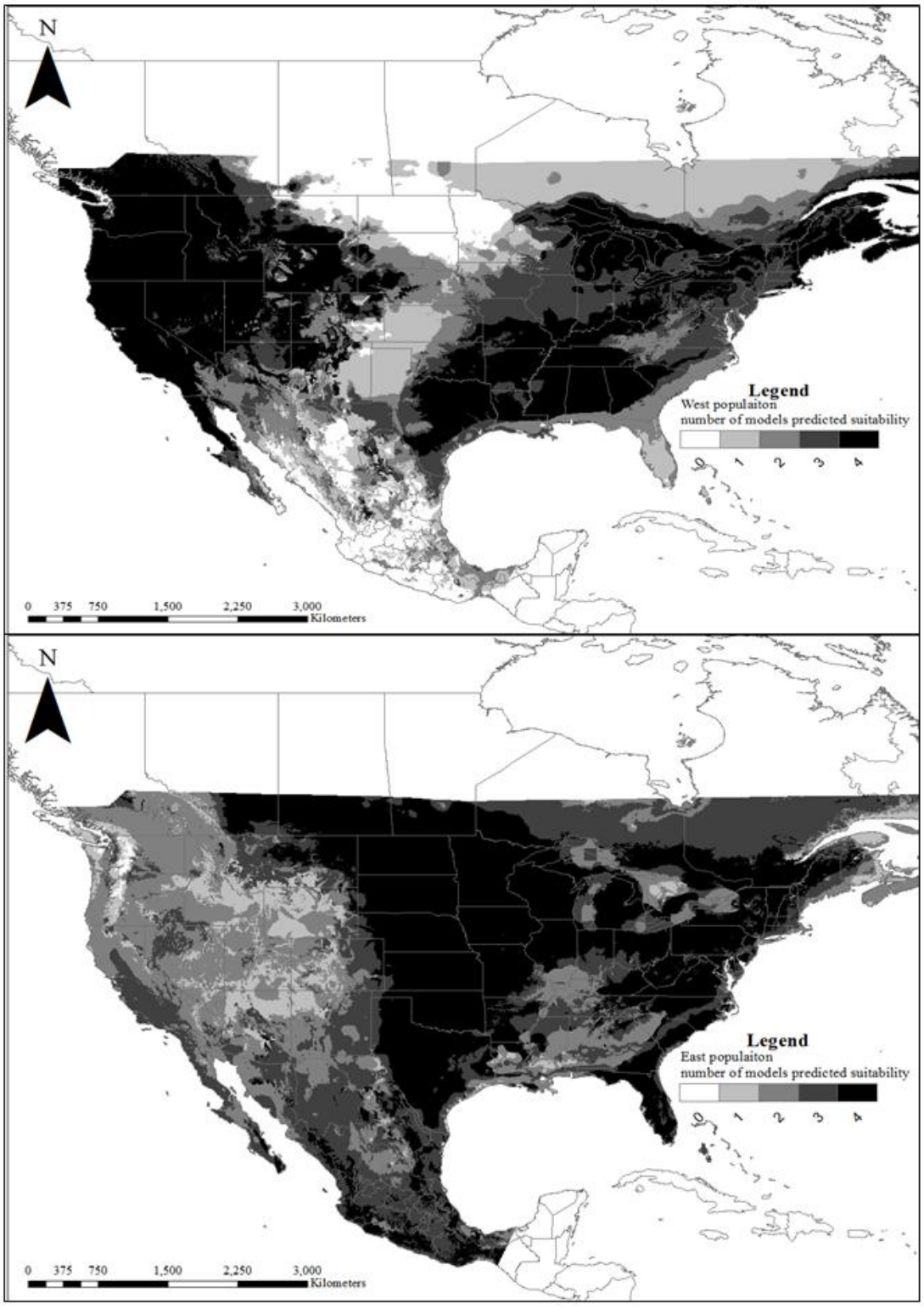
N
Legend
West populaiton
number of models predicted suitability
0 1 2 3 4
0 375 750 1,500 2,250 3,000
Kilometers
(a)
N
Legend
East populaiton
number of models predicted suitability
0 1 2 3 4
0 375 750 1,500 2,250 3,000
Kilometers
(b)

Fig. 5

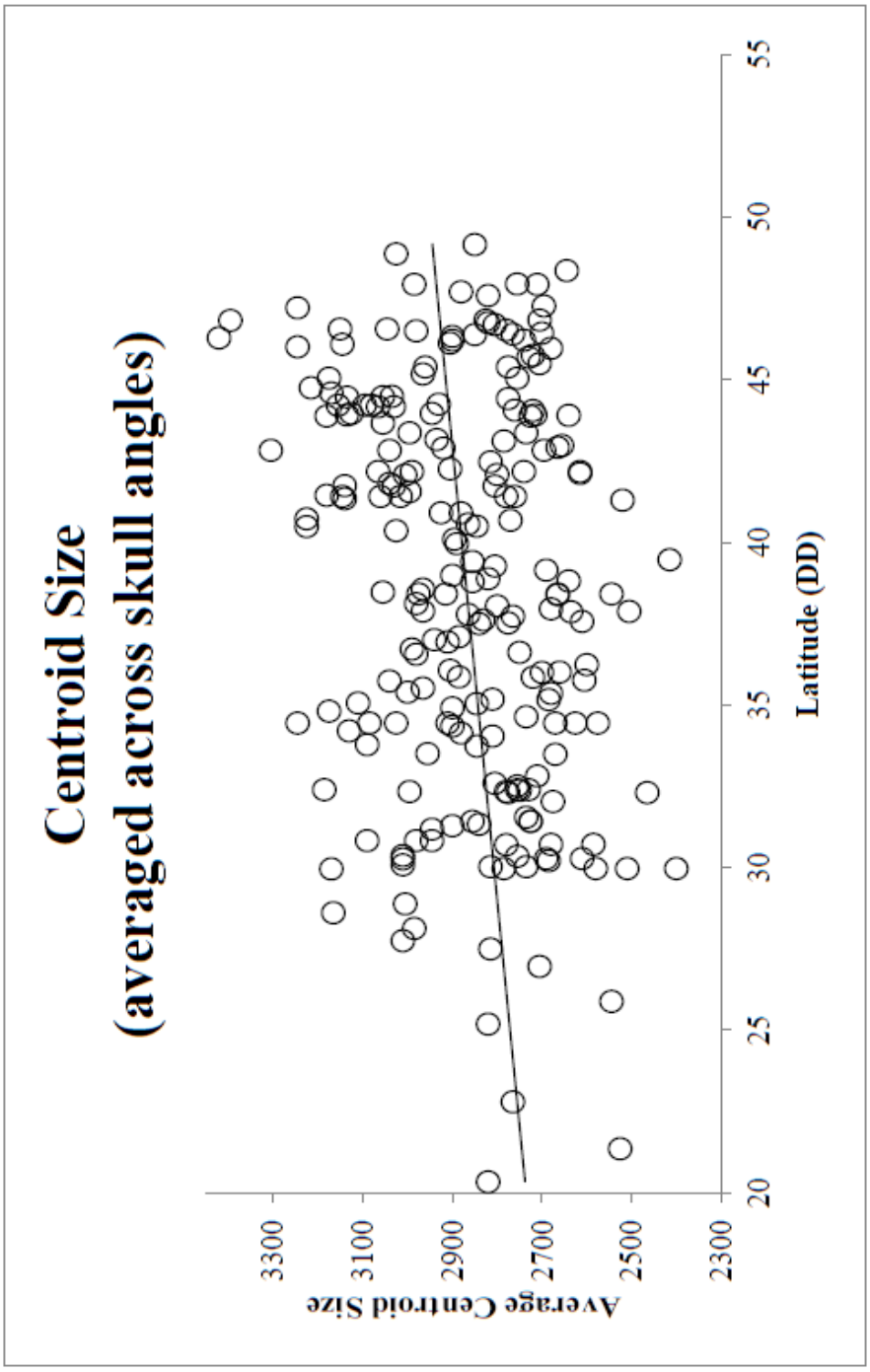
Centroid Size
(averaged across skull angles)
Average Centroid Size
3300
3100
2900
2700
2500
2300
20
25
30
35
40
45
50
55
Latitude (DD)

Fig. 6

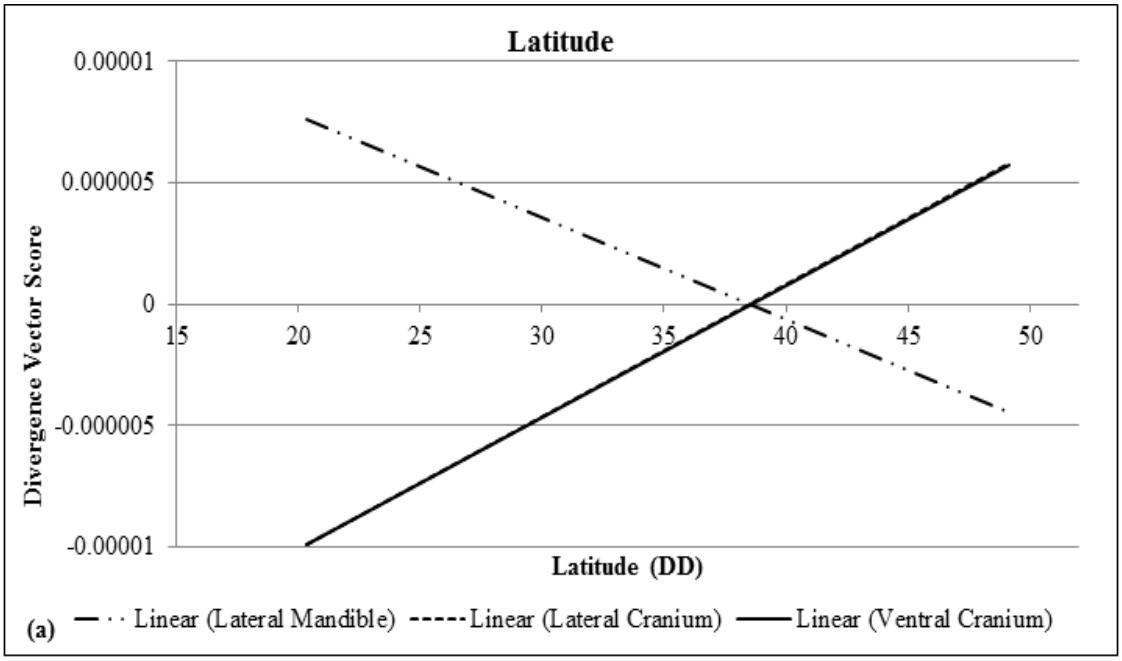

(a)

(1) Ventral Cranium

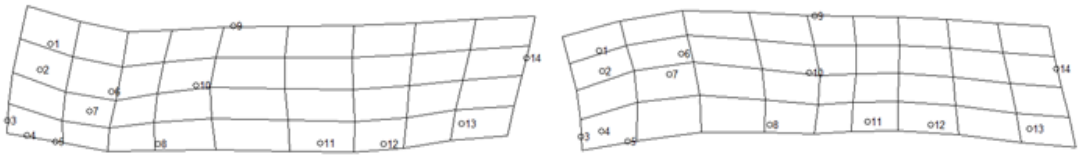

(2) Lateral Cranium

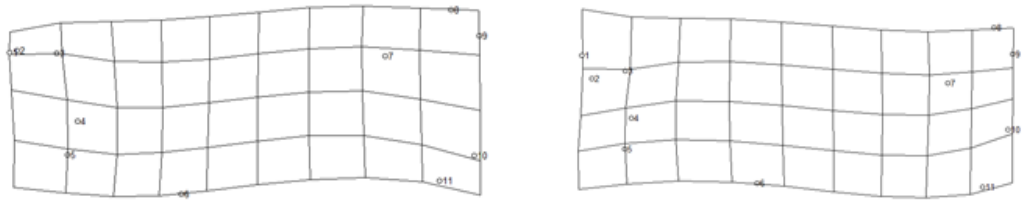

South (3) Lateral Mandible North

(b)

Fig. 7

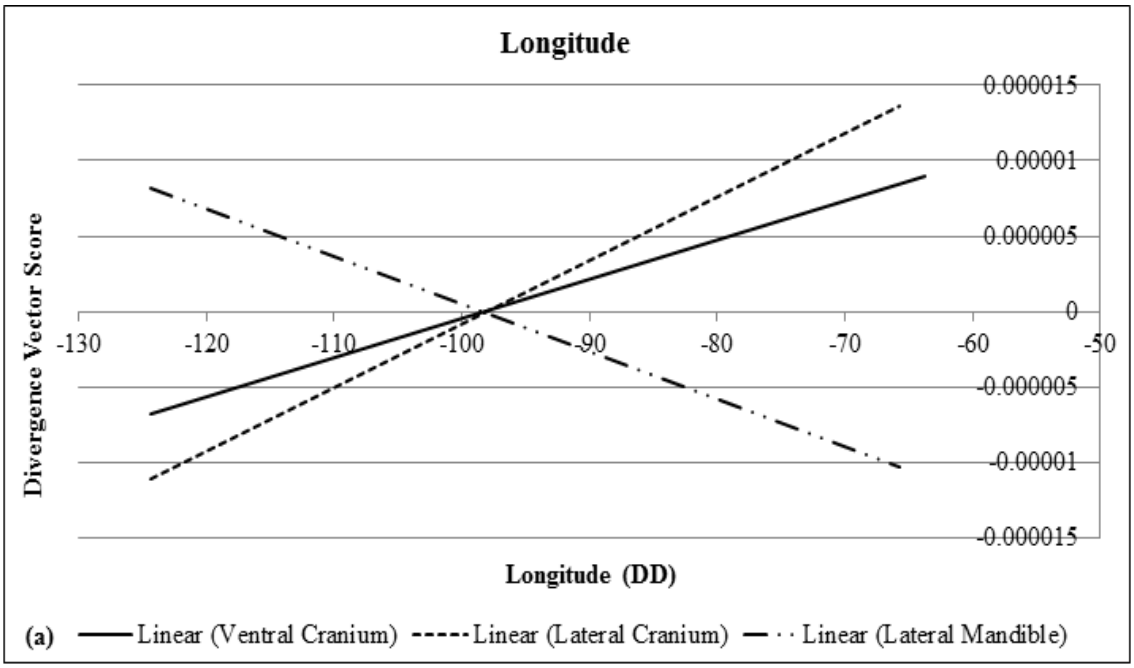

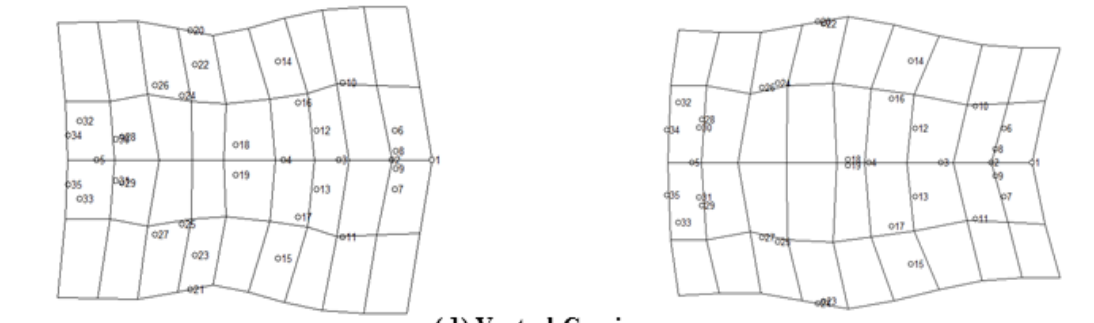

(1) Ventral Cranium

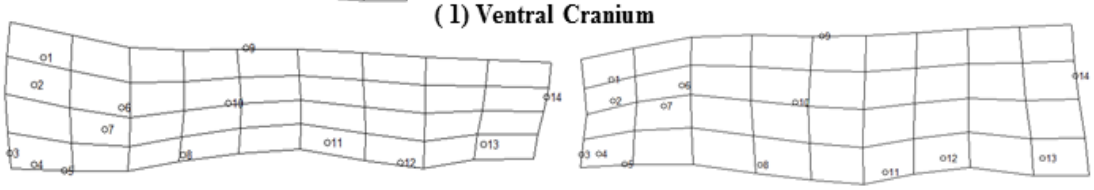

(2) Lateral Cranium

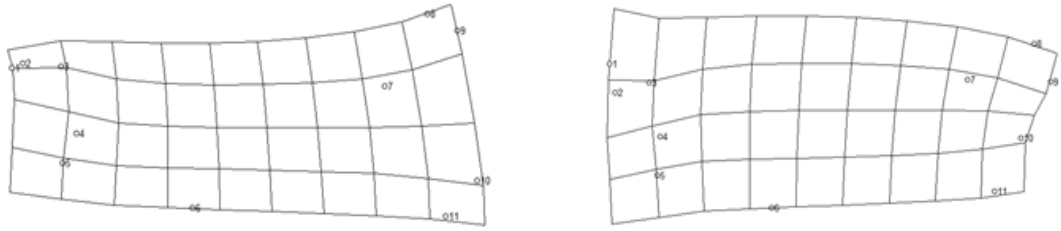

(3) Lateral Mandible

West

East

(b)

Fig. 8

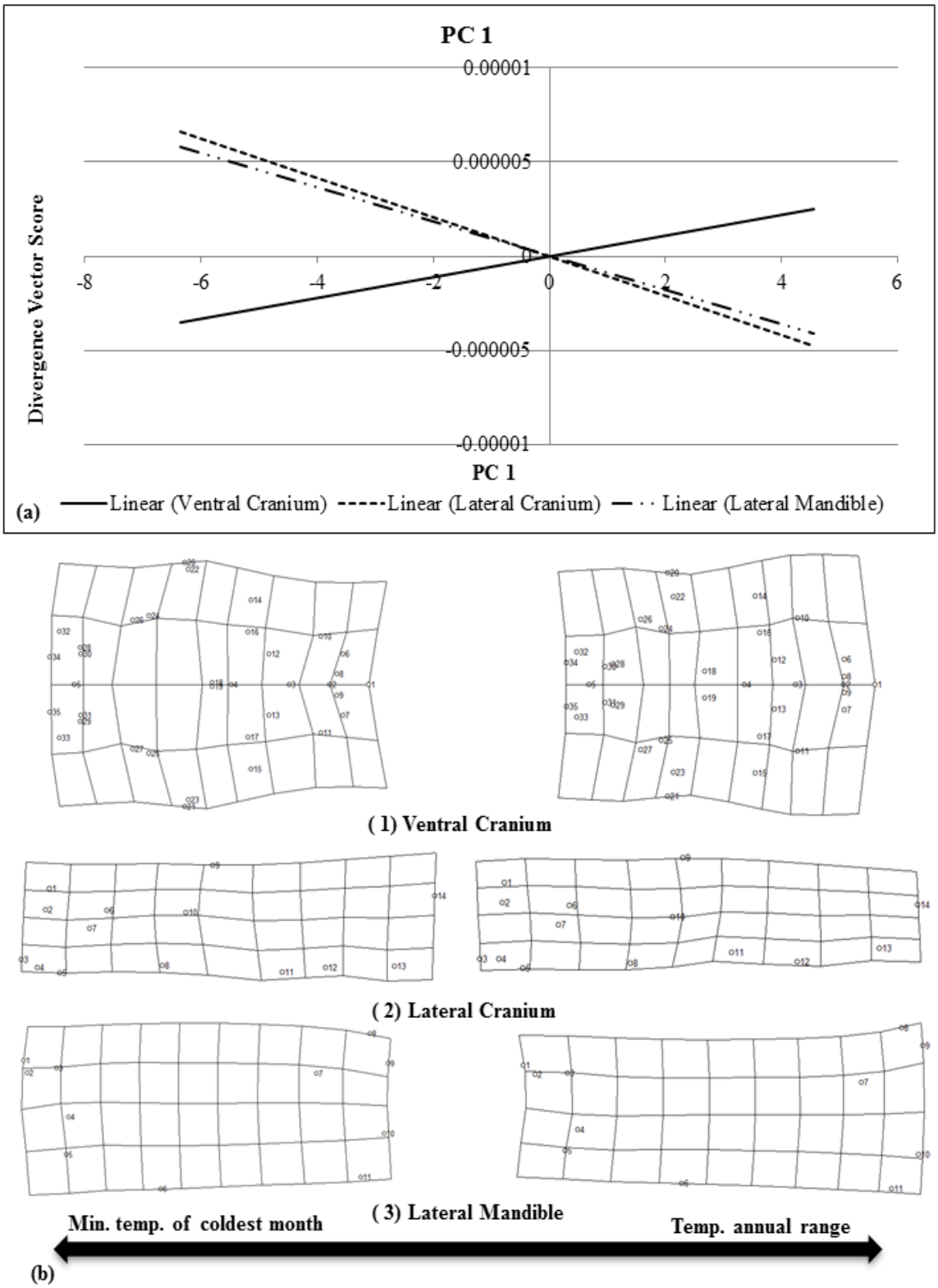
PC 1
0.00001
0.000005
-0.000005
-0.00001
Divergence Vector Score
-8
-6
-4
-2
0
2
4
6
PC 1
(a)
Linear (Ventral Cranium)
Linear (Lateral Cranium)
Linear (Lateral Mandible)
(1) Ventral Cranium
(2) Lateral Cranium
(3) Lateral Mandible
Min. temp. of coldest month
Temp. annual range
(b)

Fig. 9

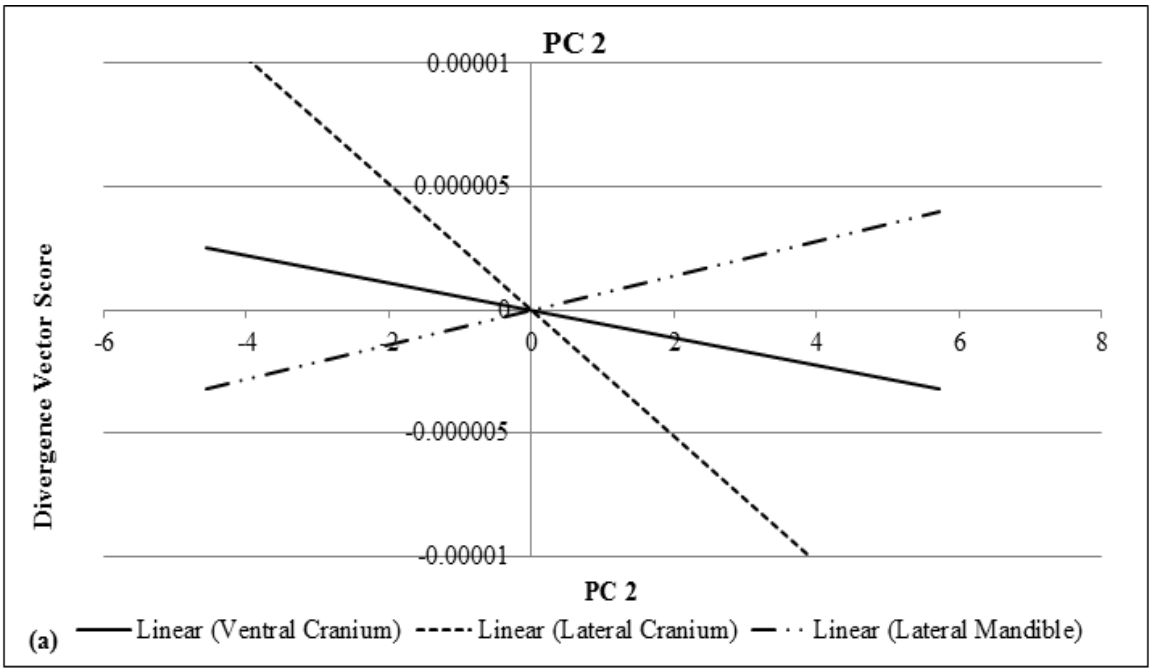
PC 2
0.00001
0.000005
0
-0.000005
-0.00001
-6
-4
-2
0
2
4
6
8
Divergence Vector Score
PC 2
(a)
Linear (Ventral Cranium)
Linear (Lateral Cranium)
Linear (Lateral Mandible)
(1) Ventral Cranium
(2) Lateral Cranium
(3) Lateral Mandible
Precip. of driest quarter
Max. temp. of warmest quarter
(b)

Fig. 10

APPENDICIES

APPENDIX S1 – **Image consistency analysis**

To determine the ability to consistently orient specimens on the image apparatus and repeatability of landmark placement, the same specimen was positioned on the image apparatus ten different times and ten pictures of the ventral angle of the cranium were collected. Using tpsDig2 version 2.17 (Rohlf, 2004; available at: http://life.bio.sunysb.edu/morph/), 21 landmarks were placed on the skull and 2 reference landmarks on a standardized ruler in each image. To quantify the amount of variation attributed to human error, I conducted a bivariate correlation on the landmark coordinates and calculated two–tailed Pearson's correlation values in SPSS, following image processing methods described in methods section (distance corrections, superimposition, and averaged across midline). Only one of the ten images was not significantly correlated with the others, 2 of 45 correlations were significant at P =0.05, 36 were significant at P=0.01, and 7 were not significant (due to one image only). TspRelw (Rohlf, 2004) was used to visualize the variation in landmark placement. All landmarks were visually consistent with the exception of landmark 5, the anterior point of the foramen magnum. This trial analysis showed that any variation due to human error during image acquisition or landmark placement were insignificant.

Table S1-1. Results of bivariate image correlation, P-values are significant at 0.05 and 0.01 (shown in bold).

Image									
1	2	3	4	5	6	7	8	9	10
.566	.566	**.020**	.207	.973	**.001**	.738	.422	.934	.912
.020	**.000**	**.000**	**.000**	**.000**	**.000**	**.000**	**.000**	**.000**	**.000**
.207	**.000**	**.000**	**.000**	**.000**	**.000**	**.000**	**.000**	**.000**	**.000**
.973	**.000**	**.010**	**.010**	**.010**	**.000**	**.000**	**.000**	**.000**	**.000**
.001	**.000**	**.000**	**.000**	**.002**	**.002**	**.002**	**.000**	**.043**	**.000**
.738	**.000**	**.000**	**.000**	**.000**	**.000**	**.000**	**.000**	**.000**	**.000**
.422	**.000**	**.000**	**.000**	**.000**	**.000**	**.000**	**.000**	**.000**	**.000**
.934	**.000**	**.000**	**.000**	**.000**	**.000**	**.000**	**.000**	**.000**	**.000**
.912	**.000**	**.000**	**.000**	**.000**	**.000**	**.000**	**.000**	**.000**	**.000**

APPENDIX S2 – **Landmark descriptions**

Table S2 – 1. Anatomical descriptions of landmarks digitized on each angle of the cranium and mandible (a) ventral cranium, (b) lateral cranium, and (c) lateral mandible.

(a) Ventral view

1 – anterior point of pre-maxilla suture
2 – premaxilla – maxilla suture
3 – maxilla – palatine suture
4 – palatine mid – line suture
5 – anterior point of foramen magnum
6, 7 – junction of canine and premaxilla – maxilla suture
8, 9 – posterior point on incisive foramen
10, 11 – ventral point on infraorbital canal
12, 13 – posterior point on palatine foramen
14, 15 – maxilla – jugal suture
16, 17 – maxilla – palatine suture
18, 19 – basisphenoid – presphenoid suture
20, 21 – posterior – lateral point jugal – squamosal suture
22, 23 – anterior, lateral edge of glenoid fossa
24, 25 – medial point of glenoid fossa
26. 27 – lateral edge of external auditory meatus
28, 29 – medial point of the jugular foramen
30, 31 – medial point of the hypoglossal canal
32, 33 – lateral point of occipital condyle
34, 35 – posterior and medial point of occipital condyle

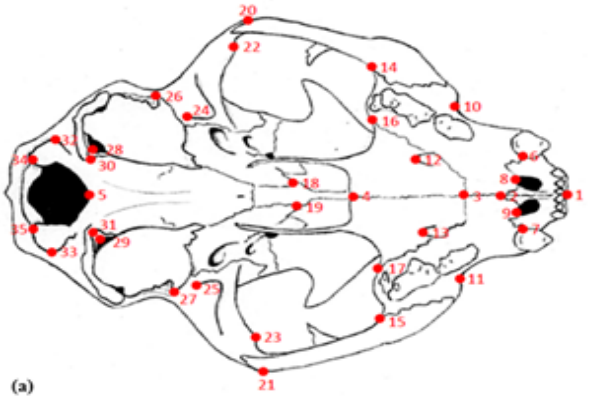

(b) Lateral view

1 – anterior most point on the nasal
2 – anterior most point on the nasal – premaxilla suture
3 – incisor meets premaxilla
4 – anterior point on canine at maxilla
5 – posterior point on canine at maxilla
6 – dorsal – most point on lacrimal foramen
7 – anterior point of jugal – maxilla suture at infraorbital foramen
8 – maxilla – jugal suture
9 – tip of postorbital process from frontal
10 – upper point of jugal – squamosal suture
11 – lower end of jugal – squamosal suture
12 – upper point of exterior auditory meatus
13 – upper point of the occipital condyle
14 – most posterior point of nuchal crest

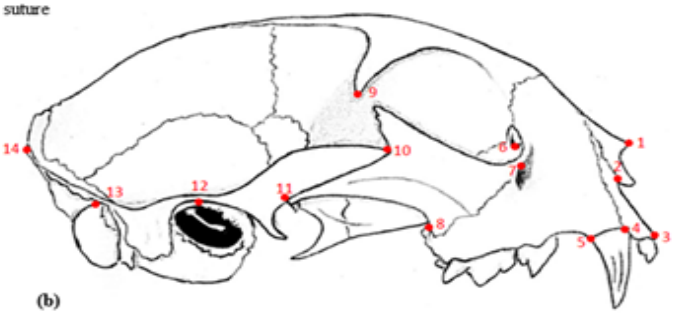

(c) Mandible view

1 – anterior point of incisor and dentary
2 – anterior most point of canine
3 – posterior most point of canine
4 – dorsal point of mental foramen
5 – mandibular symphasis
6 – ventral apex of mandible
7 – dorsal most point of massoteric fossa
8 – dorsal apex of coronoid process
9 – posterior most point of coronoid process
10 – posterior point of condyle
11 – dorsal and posterior apex of articular process

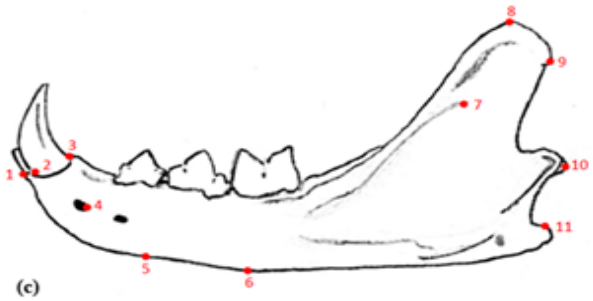

Fig. S2 -1. Cranium and mandible image angles used in this project and the anatomical locations of the landmarks that were used for the morphology analyses; (a) ventral cranium, (b) lateral cranium, and (c) lateral mandible.

APPENDIX S3 - **MANCOVA**

Table S3 -1. The results of a MANCOVA showing the effect of various parameters on skull shape variation.

Ventral Cranium (Wilks' Lambda)				
Effect	Value	F	Degrees of freedom	Significance
Intercept	0.522	4.496	36	<0.001
Centroid	0.379	8.039	36	<0.001
Latitude	0.636	2.811	36	<0.001
Longitude	0.385	7.865	36	<0.001
Collection Year	0.882	0.655	36	0.933
Sex Code	0.772	1.452	36	0.060
Lateral Cranium (Wilks' Lambda)				
Effect	Value	F	Degrees of freedom	Significance
Intercept	0.522	4.496	24	<0.001
Centroid	0.379	8.039	24	<0.001
Latitude	0.636	2.811	24	<0.001
Longitude	0.385	7.865	24	<0.001
Collection Year	0.882	0.655	24	0.933
Sex Code	0.772	1.452	24	0.060
Lateral Mandible (Wilks' Lambda)				
Effect	Value	F	Degrees of freedom	Significance
Intercept	0.522	4.496	18	<0.001
Centroid	0.379	8.039	18	<0.001
Latitude	0.636	2.811	18	<0.001
Longitude	0.385	7.865	18	<0.001
Collection Year	0.882	0.655	18	0.933
Sex Code	0.772	1.452	18	0.060

APPENDIX S4 – **Geographic pattern of divergence vector scores (DVS)**

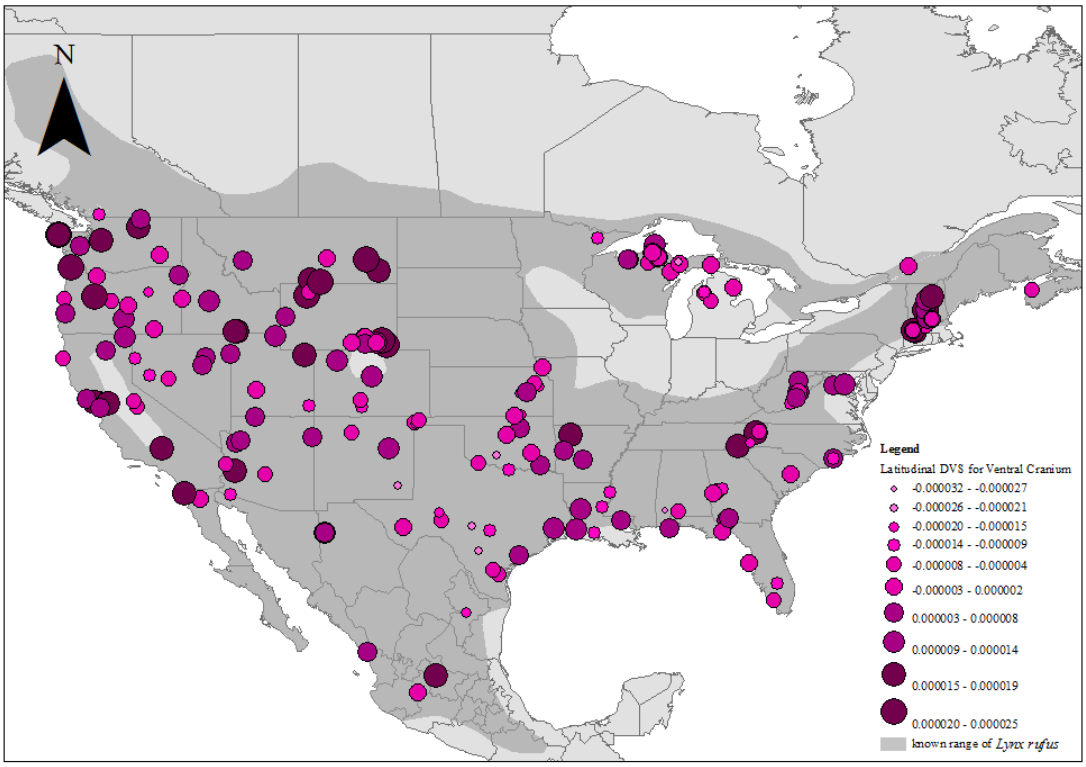

Fig. S4 – 1. Geographic distribution of divergence vector score (DVS) values for the ventral cranium created along a latitudinal trend. Similar DVS reflect similar variations in shape of the ventral cranium (also refer to Fig. 7 for linear regression; geographic coordinate system is North American 1983; range map produced by Nature Serve, Patterson et al., 2003).

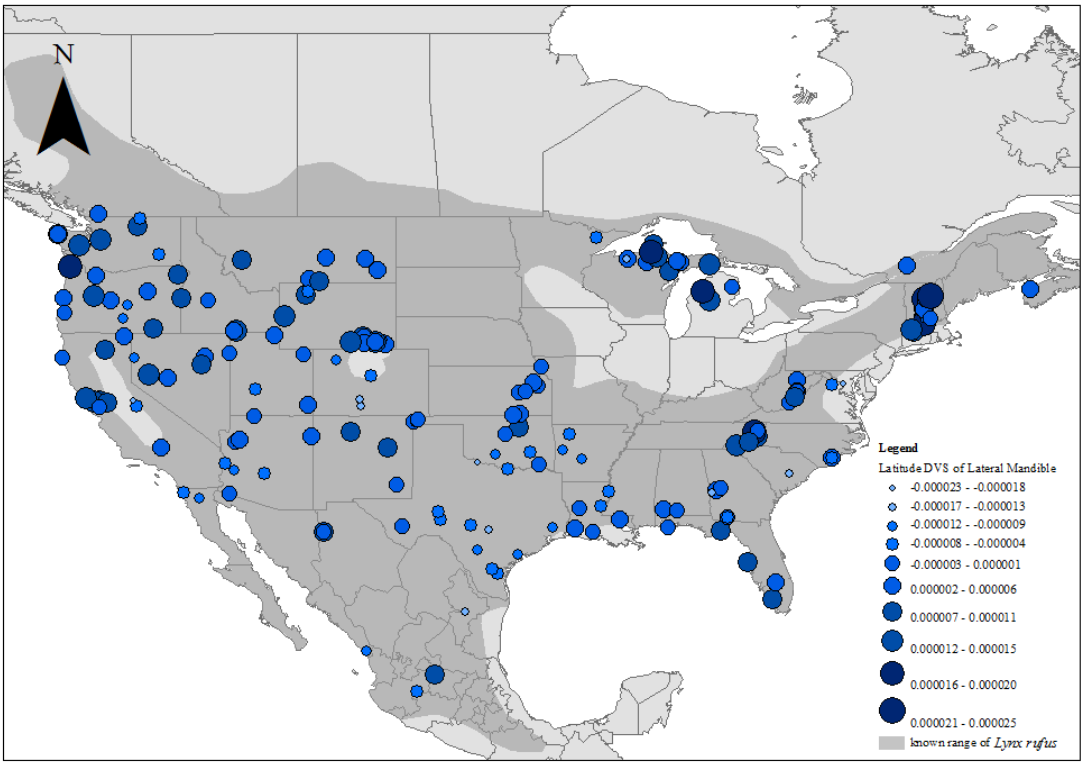

Fig. S4 – 2. Geographic distribution of divergence vector score (DVS) values for the lateral cranium created along a latitudinal trend. Similar DVS reflect similar variations in shape of the lateral cranium (also refer to Fig. 7 for linear regression; geographic coordinate system is North American 1983; range map produced by Nature Serve, Patterson et al., 2003).

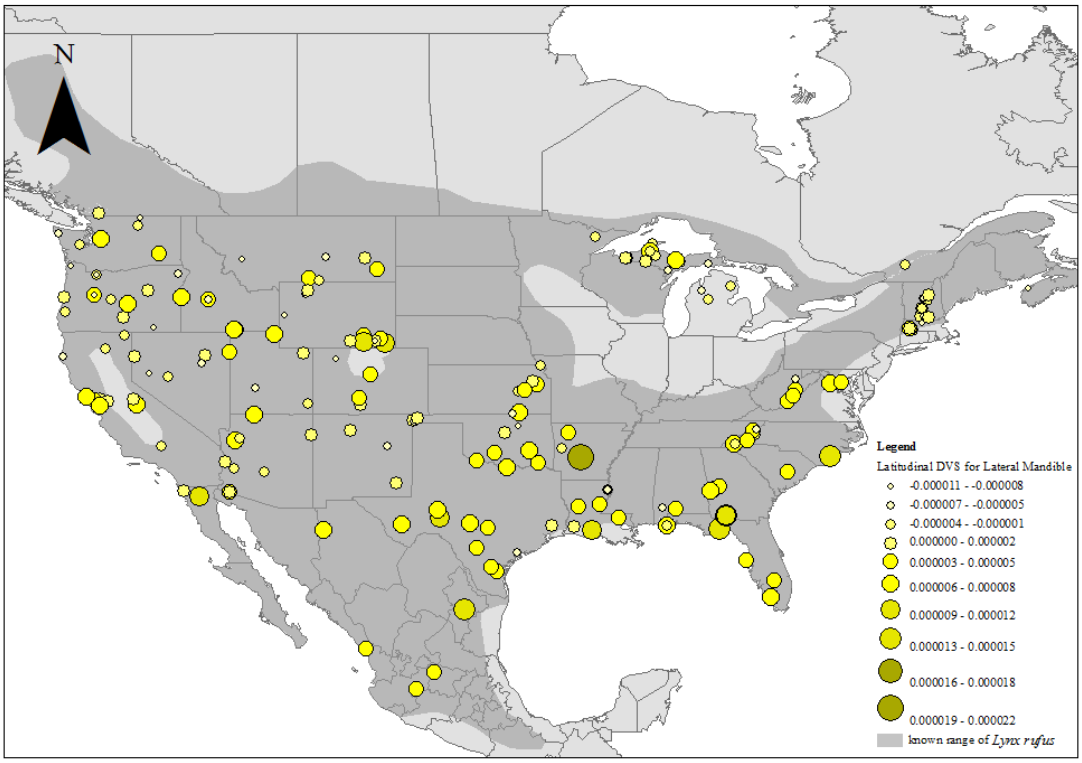

Fig. S4 – 3. Geographic distribution of divergence vector score (DVS) values for the lateral mandible created along a latitudinal trend. Similar DVS reflect similar variations in shape of the lateral mandible (also refer to Fig. 7 for linear regression; geographic coordinate system is North American 1983; range map produced by Nature Serve, Patterson et al., 2003).

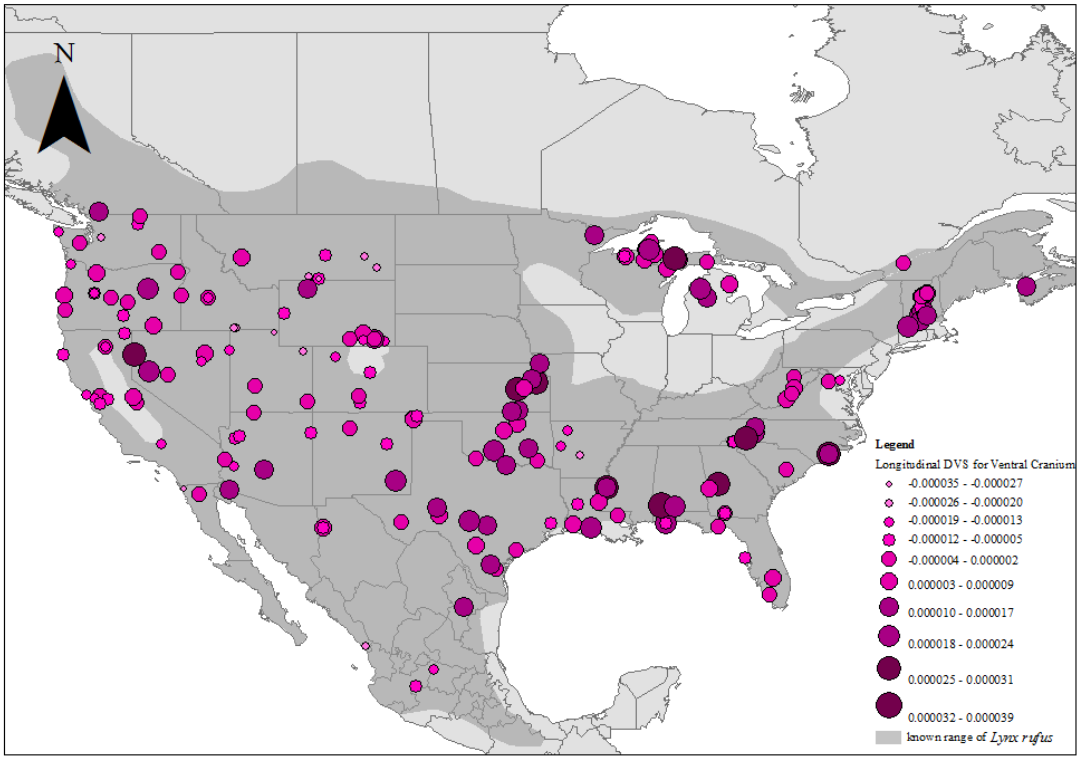

Fig. S4 – 4. Geographic distribution of divergence vector score (DVS) values for the ventral cranium created along a longitudinal trend. Similar DVS reflect similar variations in shape of the ventral cranium (also refer to Fig. 8 for linear regression; geographic coordinate system is North American 1983; range map produced by Nature Serve, Patterson et al., 2003).

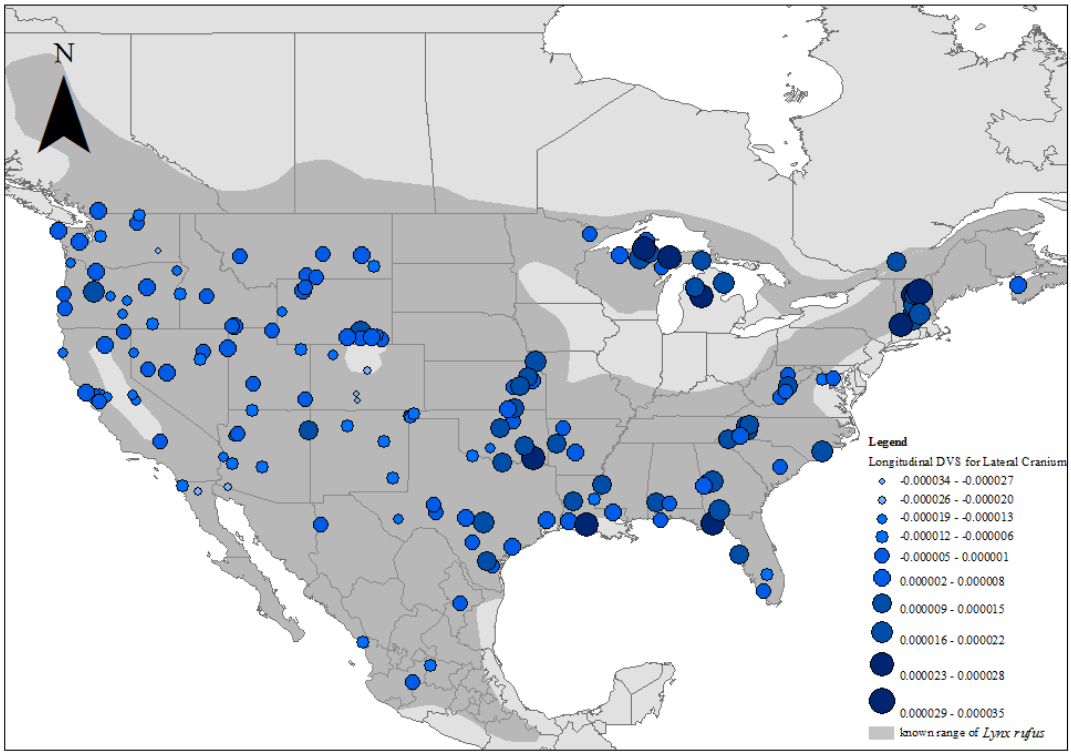

Fig. S4 – 5. Geographic distribution of divergence vector score (DVS) values for the lateral cranium created along a longitudinal trend. Similar DVS reflect similar variations in shape of the lateral cranium (also refer to Fig. 8 for linear regression; geographic coordinate system is North American 1983; range map produced by Nature Serve, Patterson et al., 2003).

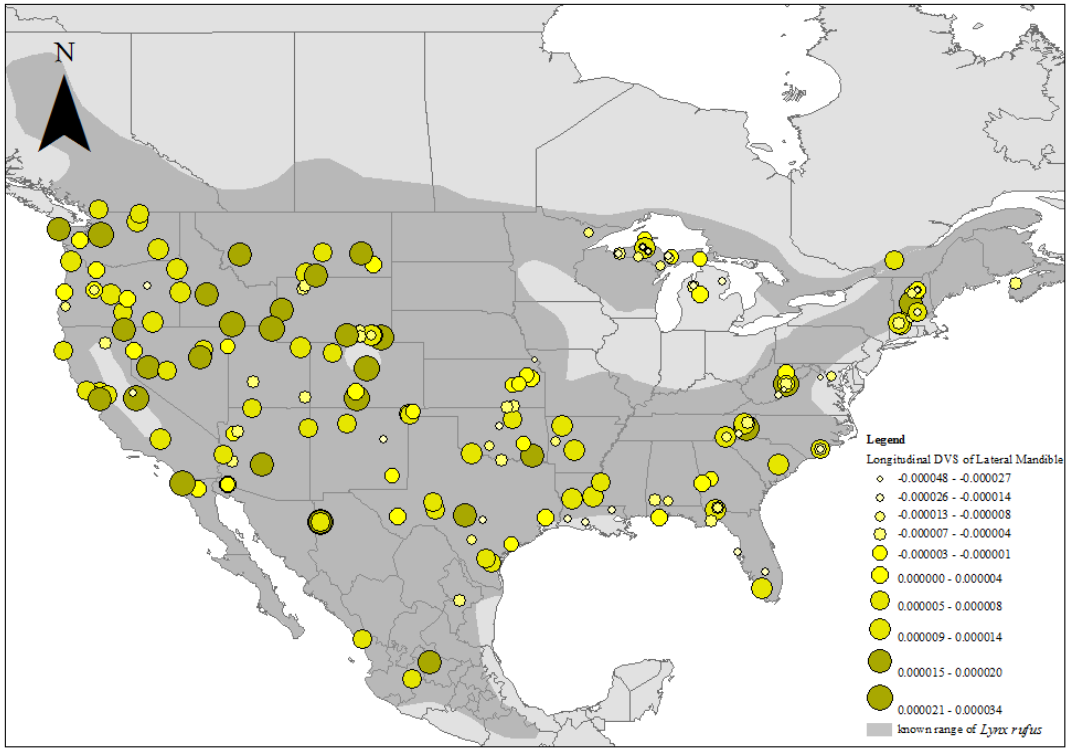

Fig. S4 – 6. Geographic distribution of divergence vector score (DVS) values for the lateral mandible created along a longitudinal trend. Similar DVS reflect similar variations in shape of the lateral mandible (also refer to Fig. 8 for linear regression; geographic coordinate system is North American 1983).

VITA

Allison Marcella Loveless

Candidate for the Degree of

Master of Science

Thesis: BOBCATS ACROSS THEIR GEOGRAPHIC RANGE: COMBINING ECOLOGICAL NICHE MODELING AND MORPHOLOGY TO ASSESS THE POPULATION GENETIC STRUCTURE OF *LYNX RUFUS*

Major Field: Zoology

Biographical:

Education:
Completed the requirements for the Master of Science in Zoology at Oklahoma State University, Stillwater, Oklahoma in December, 2014.

Completed the requirements for the Bachelor of Arts in Geography/ Environmental Studies at University of California, Los Angeles, California in 2009.

Experience:
Collection manager, Collection of Vertebrates at Oklahoma State University, Stillwater, Oklahoma, in Fall 2014
Teaching assistant for Zool 2104, Human Anatomy Laboratory at Oklahoma State University, Stillwater, Oklahoma, in Spring 2014
Teaching assistant for Biol 1114, Introductory Biology Laboratory at Oklahoma State University, Stillwater, Oklahoma, in Fall 2012 and 2013
Research assistant for Oklahoma wetland conditions EPA grant at Oklahoma State University, Stillwater, Oklahoma, in Spring and Summer 2013

Professional Memberships:
Southwestern Association of Naturalists in 2014
American Society of Mammalogists in 2014